Università degli Studi di Padova
Dipartimento di Fisica e Astronomia "Galileo Galilei"

Corso di Laurea Magistrale in
Fisica

Production of fiber-based cavities by pressing heated balls into fiber tip

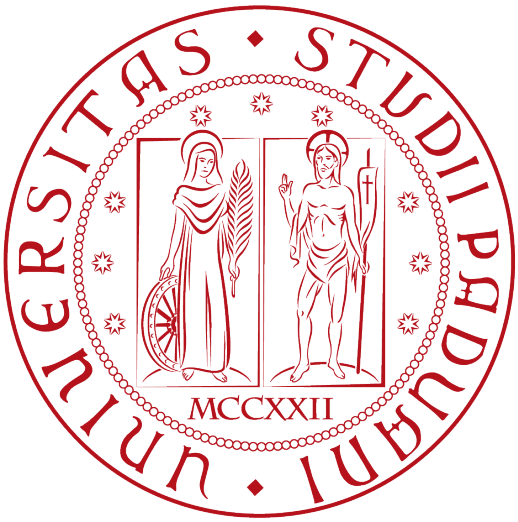

Laureando: Dario Alessandro Fioretto

Relatore: Prof. Cinzia Sada
Correlatori: Dr. Klemens Schuppert, Prof. Tracy Northup, Prof. Rainer Blatt

Anno accademico 2014-2015

11 Dicembre 2014

"Les miroirs feraient bien de refléchir un peu plus avant de renvoyer les images."

Le sang d'un poète
Jean Cocteau

Abstract

Recently it has been shown that highly reflective concave mirrors can be fabricated on optical fiber tips. These fiber mirrors can be used in high-finesse optical cavities for cavity QED experiments.
One of the main topic related with this application is to find the best technique for producing the substrate where to deposit a coating that gives adequate transmission coefficient in order to build a cavity.
The techniques used until now have been based on CO_2 laser ablation and ensure a very small surface roughness and an excellent centering.
These techniques allow us only to build cavities at most a few hundred microns in length because they give to the fiber tips a Gaussian profile, which limits the useful mirror diameter to a small area around the center. However, for integrating fiber cavities with ion traps, longer cavities are desired and thus we need a new technique to produce the mirrors.
The aim of this thesis work is to try a new method consisting of pressing a heated sphere to the fiber tip. This should guarantee a spherical shape and, after using a laser for smoothing the surface, also a very small surface roughness.
Using standard SiO_2 fibers implies the necessity to work with high temperature ($T \approx 1600°C$) near the melting point of the silica glass. In this temperature regime lots of problems arise concerning materials exploited for the building up of the setup and their thermal behaviour.
Another topic in this thesis will be the problem related the centering between the fiber and the sphere. Indeed, known optical methods are not practicable or they doesn't reach the required accuracy. So a complete new digital method has been tried.
During the thesis work it has been projected and built the setup and some preliminary results are presented.

Contents

Chapter 1

Introduction

More than a century has passed from the origin of Quantum Mechanics and lot of questions remain without an answer. A useful instrument that the physicist of that age may use is the thought experiment (Gedankenexperiment). Today, lot of things that was thought to be unrealisable are actually possible and lots of applications arises.
For example, it has been proposed [1] and proved that quantum mechanics laws may be used for implement algorithmically faster computing machine [2][3] and may allow new cryptographic systems [4].
The techniques in experimental quantum computation and quantum information are improving day by day very fast. Different implementations and new devices are proposed every day. Ion traps, cavities, superconductive junctions are only few of the tools that today an experimentalist may use to test quantum mechanics laws and to build quantum devices [13]. Cavities, which are systems of mirrors that efficiently confine the light, has very interesting properties that may be used to test very fundamental laws of nature. With the development of optics and laser technology a new branch of physics was born. It studies the interaction between the laser light confined in a cavity and atoms or ions, for example, between the two mirrors was born. This subject is called Cavity Quantum Electrodynamics (Cavity QED) [12].
Indeed it has been experimentally proved that it is possible to produce a coupling between a cavity, which is a macroscopic object, and a quantum system (for example an atom or an ion).
The basic idea of Cavity QED is that inside the cavity, light is quantized like in a infinite potential well. The atom or the ion inside may be simplified to a two level system, a ground state and an excited one. It is possible to tune the cavity in order to have the light inside resonant or nearly resonant with the atomic transition.
First experiments were done with neutral atoms. In Innsbruck University,

the team of the project led by Tracy Northup in the Prof. Blatt's Quantum optics and spectroscopy group has built a Cavity QED experiment which uses trapped ions and it is still working.
Now it has been projected a new Cavity QED experiment with trapped ions. The ions offer different advantages in these setups:

- The ions stay stably in the Paul trap for up to several days and this allows the experimentalists to work with the exact same quantum system

- The ions are well localized in the trap. These allow a really optimized coupling with an eventual cavity mode.

This aims to reach an enhancement in the strength of the coupling between ion and cavity because for building an high-fidelity ion-photon quantum interface it's necessary to have a system where the rate of spontaneous emission of ions is smaller than coupling strength [5]. In order to reach this ambitious goal it's necessary to build smaller cavities and so standard high reflectivity mirrors are not sufficient anymore.
A very promising possibility in this sense are Fiber-based Fabry-Perot cavities (FFPC). FFPCs are optical systems composed by two mirrors built on the tip of two different fibers one in front of the other. For better confine the light between these two mirrors, a concave tip is necessary but very predictable result are known only with spherical profiles.
Meanwhile the technique for depositing the coating which has the function of mirror is well known, the way that is better for producing the spherical substrate on the tip is still subject matter of the research.
It's evident that the cavity production has a major importance in the success of cavity QED experiments and in particular shaping fiber tips is a very challenging branch of applied optics.
Exploring a new alternative for the shaping of the end face of the fiber is the subject of the thesis. Indeed until now only few techniques are well known and give really promising results and everyone implies the use of a CO_2 laser for ablating the surfaces.
The main proposal with laser ablation to shape the fiber has very good results in terms of roughness and centering but with the main limit to involve in the process only a small portion of the fiber around the core.
In this thesis it will be given a proof of principle of a completely different technique for producing fiber tips that it has been experienced only few times.
This method uses spheres which are pressed onto fibers in an high temperature environment. It has been built for the really first time in Harald Glessen's group at the university of Stuttgart

1.1 Cavity QED

Cavity QED studies the coupling between the light in a cavity and a quantum system confined between these two mirrors.
It is possible to introduce light into the cavity with a laser which has a resonance frequency defined by the cavity geometry, in particular by the length.
Inside these two mirrors, for example, an atom is confined. It is possible to describe it as a two level system, a ground state $|g>$ and an excited one $|e>$.
It is possible to change the cavity length and in this way the light inside the cavity may be tuned resonant or nearly resonant with the transition between these two states. In this sense he electromagnetic field cannot be considered independently of the cavity itself. This feature - the controlled coupling of a macroscopic system (the cavity) with a small quantum system (the atom) - was only realised in thought ideal experiment. Today different setup achieved this result and it is a common quantum information experimental system. In Innsbruck different improvement to that technique has been done and here will be briefly presented.

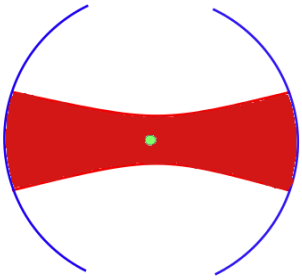

Figure 1.1: Scheme of standard Cavity QED system. Two mirrors are confining light inside them and an atom in the half is resonant to the light field.

This physical system is well described by the Jaynes-Cummings model, proposed in 1963.
The Hamiltonian that describes this kind of systems is composed by three terms and can be expressed as:

$$H = H_a + H_c + H_{ac} \tag{1.1.0.1}$$

Where H_a and H_c are the atom and the cavity Hamiltonian, respectively. The coupling Hamiltonian is H_{ac} and can be expressed as $H_{ac} = -\mathbf{D} \cdot \mathbf{E}_c$ with $\mathbf{D}$ the atomic dipole operator and $\mathbf{E}_c$ the cavity electric field at the

atom position. Assuming that the atom is at the center of the cavity this interaction term is expressed as:

$$H_{ac} = -d(\epsilon_a \sigma_- + \epsilon_a^* \sigma_+) \cdot i\Sigma_0(\epsilon_c a - \epsilon_c^* a^\dagger) \tag{1.1.0.2}$$

where it has been used the second quantization formalism. It is possible to reduce this formula to:

$$H_{ac} = \hbar g(a\sigma_+ - a^\dagger \sigma_-) \tag{1.1.0.3}$$

where:

$$g = -i\frac{d\Sigma_0 \epsilon_a^* \cdot \epsilon_c a}{\hbar} \tag{1.1.0.4}$$

is called coupling strength.
The total Hamiltonian now becomes:

$$H = \epsilon_c a^\dagger a + \epsilon_a \sigma_+ \sigma_- + \hbar g(a\sigma_+ - a^\dagger \sigma_-) \tag{1.1.0.5}$$

In this equation $a^\dagger a$ is the number operator for the photon and $\sigma_+\sigma_-$ is number operator for the electron state, ϵ_c and ϵ_a are respectively the energy of a photon in the cavity and the energy of the excited state of the atom. The term $a\sigma_+$ and $a^\dagger\sigma_-$, represent the fact that a photon can be absorbed by the electron of the atom and pass to an excited state or that an atom in excited state decay and emits a photon. This equation can be considered as one of the most important in CQED.
In order to study this system it's really important to have cavities composed by high reflectivity mirrors for guaranteeing a better confinement for light. One important implementation of this cavities is composed by two separate fibers. The end-face of these fibers is concavely shaped and their surface is deposited a coating that give to the cavities all the optical properties necessary.

1.2 Fiber cavity experiment

In Innsbruck ehe research project led by Tracy Northup is developing and studying two experiments that involve Cavity QED. Differently from other experiments in CQED that has neutral atoms as quantum system, they aim to integrate optical cavities with ion traps and to use this setup as an high-fidelity ion-photon quantum interface. Indeed ion traps are one of the most promising and well known candidates for high-fidelity quantum information processing. One of this experiments has already been built few years ago,

another one has not been completed yet.
This last one introduces different improvements to the other one and aims to explore the strong-coupling regime [5], in our case a regime in which the cavity strength g is larger than the spontaneous emission rate of the ions. In order to reach this result is necessary to minimize the cavity length and/or the cavity waist. This dependency can be derived by resolving equation 1.1.0.4 with the cavity parameters:

$$g = \frac{\lambda}{\pi w_0}\sqrt{\frac{3c\gamma_e}{L}} \tag{1.2.0.6}$$

where γ_e is the spontaneous emission rate, L the length of the cavity and w_0 the waist size in the cavity. w_0 can be written as:

$$w_0 = \frac{\lambda}{2\pi}\sqrt{L(2r - L)} \tag{1.2.0.7}$$

where r the radius of curvature of the mirrors (in a symmetric-case cavity) and λ is the wavelength of the light inside.
In order to minimize the losses the mirrors, these has to have low roughness in this experiment. Furthermore the high reflectivity coatings for the mirrors are dielectric and this property may interfere with the electromagnetic field in the trap, change the potential and so compromise the trapping itself.
A promising possibility for building this cavities, and the one the Innsbruck

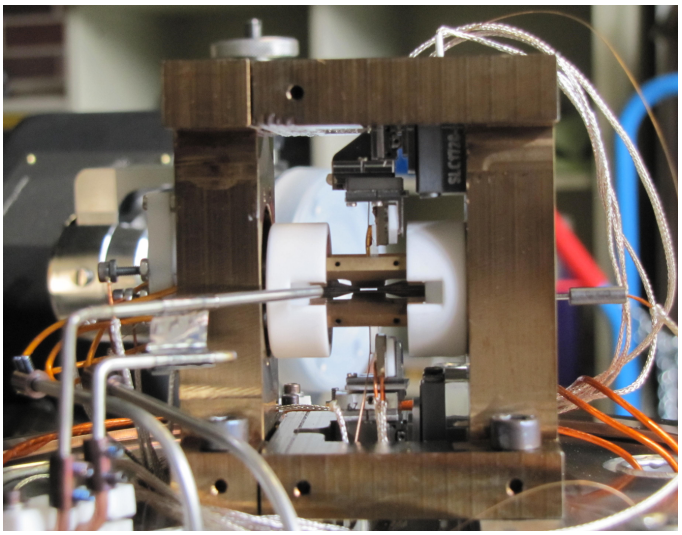

Figure 1.2: Photo of the Cavity QED experiment with fibers. In the center there is the Paul trap. It will be insert in a vacuum environment and 2 fibers will be integrated.

research group choose to pursue, is to use concave tips of two different and opposing fibers because of their dimensions and ease of integration.
One of the biggest goal that this group aims, is to connect the two cavity QED experiment and make first tests of quantum network which involves ions states.

1.3 Spherical fiber tips production

Commonly the production of fiber cavities it's done into two steps.
The first is to shape the fiber tips for giving them a concave profile. This determines all the properties of stability and confinement of the cavities.
Normally fiber optical properties (transmission coefficient) are not satisfactory for cavities and so the second step it's usually to apply an high-reflectivity coating (depending on the purpose). It is possible can reach transmission coefficient of few parts per million (ppm) and losses around of 10 ppm. From this part of the production depends the optical properties of the cavities as the finesse which is a measurable parameter which represents the quality of the confinement in the cavity.
In this section will be presented two techniques for shaping fibers. The first which uses CO_2 laser ablation and a second mechanical method, that is the topic of the thesis.

1.3.1 Laser ablation technique

The main idea for this method is to use CO_2 laser ablation for shaping the end face of the fiber.
This method has been first tried in Reichel group at ENS in Paris in 2007.
The process formerly composed by two steps. A first step of alignment of the fiber with respect to the laser focus done with a dichroic beam splitter and an optical microscope. They can reach lateral alignment precision better than 2 μm [6].
Then with a single CO_2 laser pulse the fibers are shaped. They have obtained well shaped fibers with lasers waist sizes between 18 and 80 μm, power in the range between 0.3 to 1.1 W and pulse length between 5 to 400 ms.

During this experiment they produce a large number of fiber structures (> 500). In order to obtain data on their fibers it has been necessary to do profile and roughness measurement but scanning the full surface is a very slow process. To obtain raw data about the quality of their result they choose to use an interferometric microscope which give them a measurement of the large scale ($> \lambda$) surface topography.

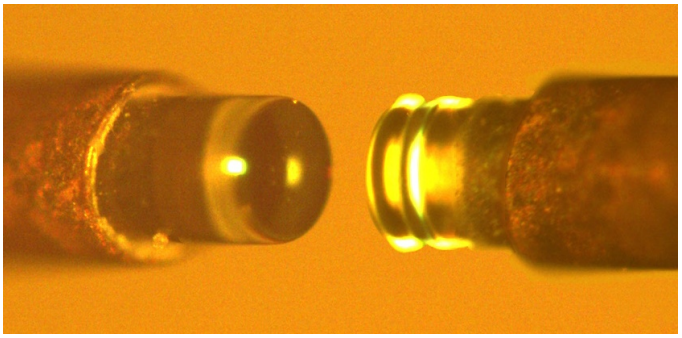

Figure 1.3: Fiber obtained with laser ablation at ENS in two different perspective. This photo is obtained merging five different photos

The results illustrated in Figure 1.4 shows that they can produce concave

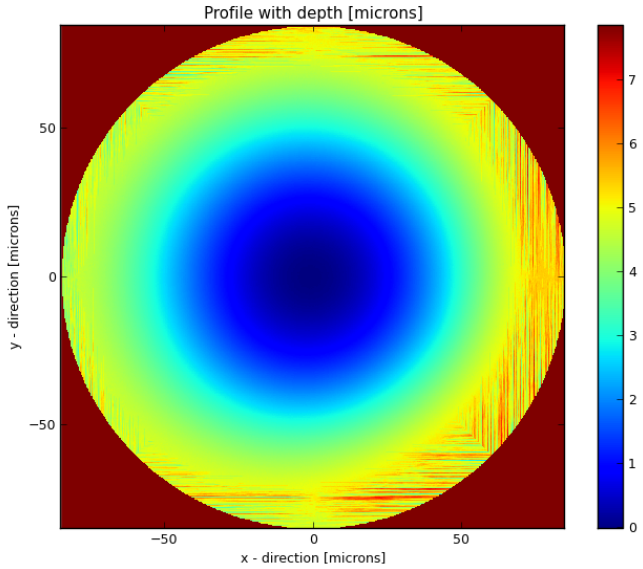

Figure 1.4: Example of profilometric measurement done at ENS in Reichel group.

spherical profile with radius of curvature between $40\mu m$ to $2\mu m$, and the surface obtained involve between 10 and $45\mu m$ of the total fiber diameter. The surface obtained has a roughness of about 0.2 nm rms.
These are optimal result in term of centering and roughness and the only problem concerns the surface shape. Indeed the result shows the profile is not spherical but has a sort of gaussian shape. This means that only a small portion of the fiber is approximately a sphere and so inside there light has a

predictable behaviour. An estimation of the useful diameter may be the full width at 1/e ($< 50\mu m$).

1.3.2 Mechanical technique

The first proposal for a not-laser based technique for manufacturing fiber tip has been carry out in Stuttgart university at Glessen's research group.
The idea, which is the same we will use in our experiment, is to produce concave fiber end face pressing fibers onto the surface of heated balls [11]. In this way, the surface involved in the process is the complete tip and it should solve the limited size of the spherical shape achieved by the laser ablation technique.
The setup was done with a ceramic holder for the fiber and a tube that kept fixed by suction the sphere and was moved by a three-axis piezo stage. A resistive heater will provide to reach high temperatures.
The used fibers weren't standard, they were in Bismute oxide (Bi_2O_3) which has the particular feature of a low melting point (570° C). This allows to work with more common temperature but on the other hand it is known that this kind of fiber are really fragile and difficult to handle. The sphere is in tungsten carbide (WC) which has the melting point between 2785 and 2830° C.
The production process was carried out as follows:

1) The fiber was prepared and mounted

2) The sphere was cleaned with an ultrasonic bath in isopropanol and mounted onto the ceramic tube

3) The light from a 10 mW laser diode ($\lambda = 780nm$) is coupled inside the fiber and fiber is align to the center of the sphere.

4) The preheated heater was slid to the working region and after 8 seconds the fiber was ready to be imprinted with the sphere

5) The sphere was moved with the translational stage until it touched the end face of the fiber and produced a slight indention

6) In two second it is possible to remove the heater and waiting for the cooling down.

The obtained end face of the fibers and the surface of the used sphere was analysed with a white light interferometer.
To have a fast and immediate feedback about the quality of this substrates

they normally studied properties of a plano-spherical cavity built with the shaped fiber on one side and on the other side with a flat dielectric mirror with a reflectivity of 99.8%. With this asymmetric cavity the finesse was determined. Higher finesse means that surfaces are better because light cannot be scattered by imperfections.
The result shows some limit in terms of quality of the surface. Indeed the finesse obtained is $F = 2.4 \pm 0.8$. It is important to remember that this result is obtained with an uncoated fiber mirror which has a measured reflectivity $R = 0.09 \pm 0.06$. The addition of an high reflectivity coating it may arrive to $F \approx 1000$ which is in any case lower than the one obtained with the previous technique. The result in the end is completely unsatisfactory if their aim is to build an high reflectivity cavity which has typical finesse $F > 100000$.

Chapter 2

Theoretical part

2.1 Introduction into beam optics

Waves with wavefronts which are normal to an axis and with a small angle spread are called paraxial waves. We can describe this wave with the complex amplitude:

$$U(\mathbf{r}) = A(\mathbf{r}) \exp(-ikz) \tag{2.1.0.1}$$

which is a plane wave $\exp(-ikz)$ modulated by a slowly varying function of position $A(\mathbf{r})$. They satisfy the paraxial Helmholtz equation:

$$\nabla_T^2 A - i2k\frac{\partial A}{\partial z} = 0 \tag{2.1.0.2}$$

where $\nabla_T^2 = \frac{\partial^2}{\partial x^2} + \frac{\partial^2}{\partial y^2}$.
The solution of the paraxial Helmholtz equation is:

$$A(\mathbf{r}) = \frac{A_1}{q(z)} exp\left[-ik\frac{\rho^2}{2q(z)}\right] \tag{2.1.0.3}$$

with $\rho^2 = x^2 + y^2$, $q(z) = z + iz_0$ and z_0 as the Rayleigh range.

It is used conventionally to separate real and imaginary part in the expression of $\frac{1}{q(z)}$:

$$\frac{1}{q(z)} = \frac{1}{R(z)} - i\frac{\lambda}{\pi W^2(z)} \tag{2.1.0.4}$$

where:

$$W(z) = W_0 \left[1 + \left(\frac{z}{z_0}\right)^2\right]^{\frac{1}{2}} \tag{2.1.0.5}$$

$$R(z) = z \left[1 + \left(\frac{z_0}{z}\right)^2\right] \tag{2.1.0.6}$$

$$W_0 = \left(\frac{\lambda z_0}{\pi}\right)^{\frac{1}{2}} \tag{2.1.0.7}$$

Substituting, we obtain a complex amplitude:

$$U(\mathbf{r}) = A_0 \frac{W_0}{W(z)} \exp\left[-\frac{2\rho^2}{W^2(z)}\right] \exp\left[-ikz - jk\frac{\rho^2}{2R(z)} + i\zeta(z)\right] \tag{2.1.0.8}$$

with $\zeta(z) = \arctan(\frac{z}{z_0})$.
Now it is possible to calculate the intensity as $I(\mathbf{r}) = |U(\mathbf{r})|^2 = |A(\mathbf{r})|^2$:

$$I(\rho, z) = I_0 \left[\frac{W_0}{W(z)}\right]^2 \exp\left[-\frac{2\rho^2}{W^2(z)}\right] \tag{2.1.0.9}$$

where $I_0 = \left|\frac{A_1}{jz_0}\right|^2$. It is immediate now to identify $W(z)$ as a measure of the beam width because it is proportional to the width of intensity distribution, and W_0 with his minimum value and it is called waist radius.

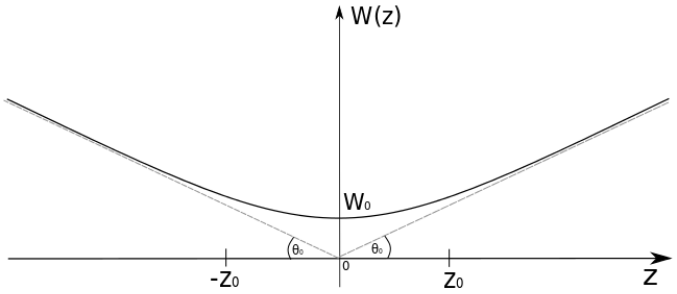

Figure 2.1: Plot of the W(z) function. It is shown in this picture also the beam divergence θ_0 and the depth of focus z_0

When $z \gg z_0$, $W(z)$ is approximately linear and it can be written as $W(z) \approx \theta_0 z$ where $\theta_0 = W_0/z_0$ and it's called beam divergence. On the other hand, z_0 can be identified with the depth of focus or in other words the axial distance within which the beam radius is $\sqrt{2}$ times the minimum value.

2.2 Fabry-Perot cavity

Fabry-Perot cavities (FPC) are optical cavities where light is stored between two high reflectivity mirrors M_1 and M_2.
This kind of system are ubiquitous in optics. FPCs are used, for example, for reducing the linewidth of a laser or for a stable frequency reference. These cavities are exploited in lots of lasers device and they are one of the most important parts in CQED experiments.
Two sets of quantities characterize this kind of systems:

1) Geometrical properties of the cavity

   - The distance L between the mirrors
   - The radius of curvature ρ_1 and ρ_2 of the mirrors

2) Optical properties of the mirrors

   - The reflectivity (R_1 and R_2) and the transmittance (T_1 and T_2) of the mirrors
   - The losses of the mirrors due to some imperfection on it and of the medium material between them

2.2.1 Transmitted intensity

In order to understand how this quantities are related in FPC it's suitable to use the general scheme in Figure 2.2.

In general it is possible to model the losses of the cavity with the central optical element with a transmittance T_3 but no reflectivity. This will take account of the two principal sources of loss which are [7]:

- Losses caused by absorption and scattering in the medium between the mirrors
- Losses caused by imperfect reflection at the mirrors.

It is possible to define the half round-trip phase factor as [7]

$$\delta = \frac{\omega L}{c} \tag{2.2.1.1}$$

Let's call z the travelling axis of the incoming electric field E_0 and assume it as a plain wave. Then we can write it as:

$$\vec{E}_0(z,t) = E_0 e^{i(\omega t - kz)} \hat{e}_{x,y} \tag{2.2.1.2}$$

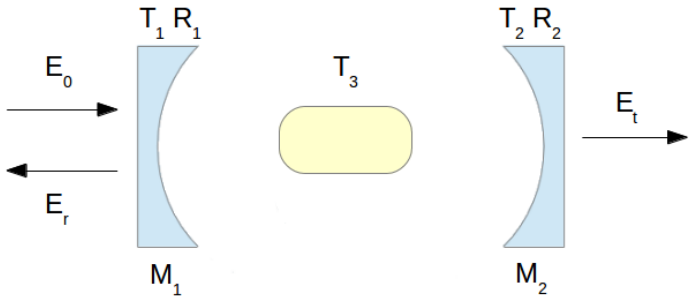

Figure 2.2: Scheme of a Fabry-Perot Cavity. It is composed by two mirrors M_1 and M_2 one in front of the other. Both the mirrors are characterized by a transmittivity and reflectivity R and T. In the half losses are modellized as an adding transmittivity T_3. E_0, E_r and E_t are respectively the intial electric field, and the reflected and transmitted one

where E_0 is the amplitude, $\hat{e}_{x,y}$ gives the polarization direction and $k = \frac{\omega}{c} = \frac{2\pi}{\lambda}$ is the module of the wave vector. The intensity related to this electric field therefore the incoming intensity inside the cavity is:

$$I_0 = \frac{\epsilon_0 c}{2} \left\langle \left| \vec{E}(z,t) \right|^2 \right\rangle_T = \epsilon_0 c \frac{E_0^2}{2} \tag{2.2.1.3}$$

and it doesn't depend on space or time respectively.
Summing up all the transmission contribution in every round-trip it is possible to obtain the transmitted electric field[8][9]:

$$\begin{aligned} E_t &= E_0 \sum_{m=0}^{\infty} \sqrt{T_1 T_2} T_3^{(2m+1)/2} (R_1 R_2)^{m/2} e^{-i\delta(2m+1) - i2\pi m} \\ &= E_0 \sqrt{T_1 T_2 T_3} e^{-i\delta} \sum_{m=0}^{\infty} (T_3 \sqrt{R_1 R_2} e^{-i2\delta - i2\pi})^m \end{aligned} \tag{2.2.1.4}$$

and using the geometrical series

$$\sum_{m=0}^{\infty} z^m = \frac{1}{1-z} \qquad \text{For } |z| \leq 1 \tag{2.2.1.5}$$

the equation becomes

$$E_t = E_0 \frac{\sqrt{T_1 T_2 T_3} e^{-i\delta}}{1 - T_3 \sqrt{R_1 R_2} e^{-i2\delta}} \tag{2.2.1.6}$$

The transmitted intensity is proportional to the square modulus of the electric field:

$$\begin{aligned} I_t &= \frac{\epsilon_0 c}{2}\left\langle \left|\vec{E}_t(z,t)\right|^2 \right\rangle_T \\ &= \frac{\epsilon_0 c}{2}\left\langle \left| E_0 \frac{\sqrt{T_1T_2T_3}e^{-i\delta}}{1-T_3\sqrt{R_1R_2}e^{-i2\delta}} \right|^2 \right\rangle_T \\ &= I_0 \frac{T_1T_2T_3}{1+T_3^2R_1R_2-2T_3\sqrt{R_1R_2}\cos 2\delta} \\ &= I_0 \frac{T_1T_2T_3}{(1-T_3\sqrt{R_1R_2})^2+4T_3\sqrt{R_1R_2}\sin^2(\delta)} \end{aligned} \tag{2.2.1.7}$$

Where we have used the goniometric property $\sin^2(\alpha) = \sqrt{\frac{1-\cos(2\alpha)}{2}}$ It's simple, with a similar procedure, to obtain the reflected electric field and intensity:

$$\begin{aligned} E_r &= E_0\left(\sqrt{R_1} - \frac{T_1T_3\sqrt{R_2}e^{-i2\delta}}{1-T_3\sqrt{R_1R_2}e^{-i2\delta}}\right) \\ I_r &= I_0\frac{(\sqrt{R_1}(1-T_3\sqrt{R_1R_2})-T_1T_3\sqrt{R_2})^2}{(1-T_3\sqrt{R_1R_2})^2+4T_3\sqrt{R_1R_2}\sin^2(\delta)} + \\ &+ I_0\frac{(4T_3\sqrt{R_1R_2}(T_1+R_1)\sin^2(\delta)}{(1-T_3\sqrt{R_1R_2})^2+4T_3\sqrt{R_1R_2}\sin^2(\delta)} \end{aligned} \tag{2.2.1.8}$$

In the case of no losses and equal mirrors ($T_3 = 1$ and $R_1 = R_2$) we can write I_r and I_t as:

$$\begin{aligned} I_r &= I_0\frac{(\frac{2\sqrt{R}}{1-R})^2\sin^2(\delta)}{1+(\frac{2\sqrt{R}}{1-R})^2\sin^2(\delta)} = I_0\frac{(\frac{2F}{\pi})^2\sin^2(\delta)}{1+(\frac{2F}{\pi})^2\sin^2(\delta)} \\ I_t &= I_0\frac{1}{1+(\frac{2\sqrt{R}}{1-R})^2\sin^2(\delta)} = I_0\frac{1}{1+(\frac{2F}{\pi})^2\sin^2(\delta)} \end{aligned} \tag{2.2.1.9}$$

with $F = \frac{\pi\sqrt{R}}{1-R}$. It's important to notice that with no losses $I_r + I_t = I_0$ as expected.

2.2.2 Essential parameters of a cavity

In this section three important parameters, which characterise the quality of a FPC, will be derived. These, as it's possible to see in Figure 2.3

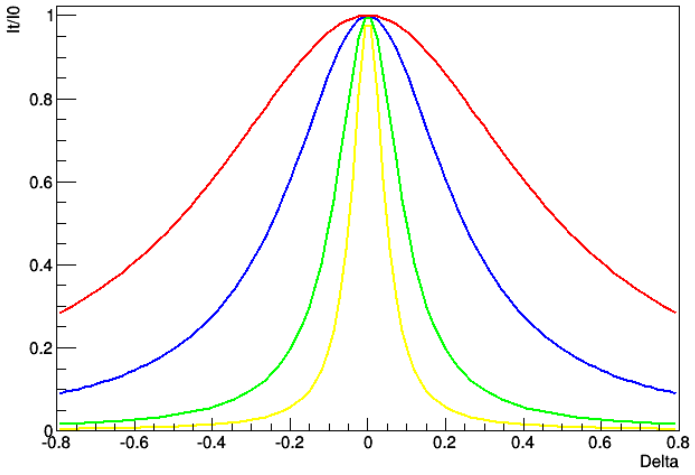

Figure 2.3: Transmitted intensity in a resonator with no losses with different finesse values. In red F = 10, in blue = 20, in green = 50, in yellow = 100

these parameter will be the distance between two adjacent peaks, which is called Free Spectrum Range (FSR), the linewidth of the peaks and the finesse [7][8][9].
From Equation 2.2.1.7 the FSR is:

$$FSR = \frac{c}{2L} \tag{2.2.2.1}$$

It is possible to characterize the linewidth of a peaks with its FWHM (Full Width Half Maximum). In order to know it is necessary to solve the equation:

$$\frac{I_t^{max}}{2} = I_0 \frac{T_1 T_2 T_3}{(1 - T_3\sqrt{R_1 R_2})^2 + 4T_3\sqrt{R_1 R_2}\sin^2(\frac{\pi}{FSR} f_{1/2})} \tag{2.2.2.2}$$

The solution will be:

$$f_{1/2} = \pm \frac{FSR}{2\pi} \arccos\left(1 - \frac{(1 - T_3\sqrt{R_1 R_2})^2}{2T_3\sqrt{R_1 R_2}}\right) + n\ FSR \tag{2.2.2.3}$$

with n integer. It is simple now to see that the FWHM is the distance between these two solutions:

$$FWHM = \frac{FSR}{\pi} \arccos\left(1 - \frac{(1 - T_3\sqrt{R_1 R_2})^2}{2T_3\sqrt{R_1 R_2}}\right) \tag{2.2.2.4}$$

Finally the Finesse F is defined as the ratio between the FSR and the FWHM:

$$F = \frac{FSR}{FWHM} = \frac{\pi}{\arccos\left(1 - \frac{(1-T_3\sqrt{R_1R_2})^2}{2T_3\sqrt{R_1R_2}}\right)} \tag{2.2.2.5}$$

This formula it's very complex to use and sometimes it may be useful to approximate it. For example if, as it commonly happens, $T_3\sqrt{R_1R_2} \approx 1$ then $\frac{(1-T_3\sqrt{R_1R_2})^2}{2T_3\sqrt{R_1R_2}}$ is small and it legitimate a Taylor expansion. The result of this expansion is:

$$F \approx \frac{\pi\sqrt{T_3\sqrt{R_1R_2}}}{1 - T_3\sqrt{R_1R_2}} \tag{2.2.2.6}$$

This definition may allow to estimate the coefficient T_3 and understand the quality of the mirror. If we approximate this formula in the symmetric ideal case ($T_3 = 1$ and $R_1 = R_2 = R$) then we obtain the F factor introduced in 2.2.1.9:

$$F = \frac{\pi\sqrt{R}}{1 - R} \tag{2.2.2.7}$$

2.2.3 Ray and beam confinement

It's very complicated to build cavities with planar mirrors because they are very sensitive to misalignment (of the light beam and of the mirrors). In contrast, Spherical-mirror (or in general concave-mirror) cavities provide a more stable configuration under certain geometrical conditions [7].

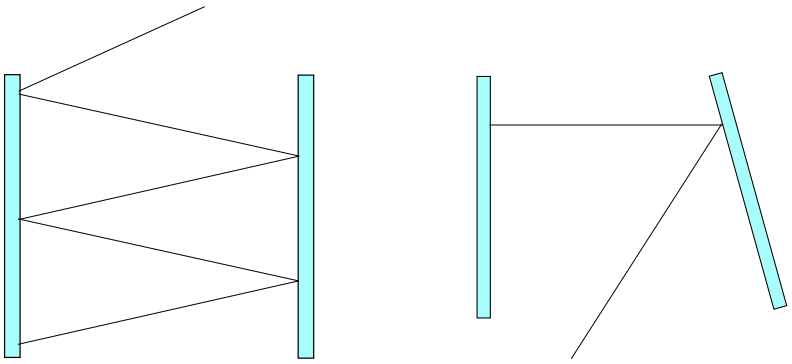

Figure 2.4: Example of misalignment in planar mirror cavity. a) is an example of the effect in a cavity of a ray misalignment. b) instead is an example of mirror misalignment. In both cases the light ray goes out of the cavity.

In order to study what happens in the case of a cavity with spherical mirrors we are going to use the ray transfer matrix formalism. It's known that in paraxial condition we can write the recursive matrix equation for a round trip:

$$\begin{pmatrix} y_{m+1} \\ \theta_{m+1} \end{pmatrix} = \begin{bmatrix} A & B \\ C & D \end{bmatrix} \begin{pmatrix} y_m \\ \theta_m \end{pmatrix} \tag{2.2.3.1}$$

Where y_m is the position and θ_m the slope of the ray. In our case:

$$\begin{bmatrix} A & B \\ C & D \end{bmatrix} = \begin{bmatrix} 1 & 0 \\ \frac{2}{\rho_1} & 1 \end{bmatrix} \begin{bmatrix} 1 & L \\ 0 & 1 \end{bmatrix} \begin{bmatrix} 1 & 0 \\ \frac{2}{\rho_2} & 1 \end{bmatrix} \begin{bmatrix} 1 & L \\ 0 & 1 \end{bmatrix} \tag{2.2.3.2}$$

where, from the left, the first and the the third matrices are the reflection through the mirrors and the others are propagation through free space.
In general, if we solve the equation, we obtain $y_m = y_{max} F^m \sin(m\phi + \phi_0)$, with $F^2 = AD - BC$, $\phi = \cos^{-1}(b/F)$, $b = (A+B)/2$. In our particular case $F^2 = 1$ by the Binet theorem. In order to be harmonic and so bounded, ϕ should exist and be real and then $-1 < b < 1$. So:

$$b = 2\left(1 + \frac{L}{\rho_1}\right)\left(1 + \frac{L}{\rho_2}\right) - 1 \Rightarrow \; 0 \leq \left(1 + \frac{L}{\rho_1}\right)\left(1 + \frac{L}{\rho_2}\right) \leq 1 \tag{2.2.3.3}$$

It is conventional to write down this condition using the parameter $g_1 = \left(1 + \frac{L}{\rho_1}\right)$ and $g_2 = \left(1 + \frac{L}{\rho_2}\right)$. Then we obtain an easier formula:

$$0 \leq g_1 g_2 \leq 1 \tag{2.2.3.4}$$

When this condition isn't satisfied, ϕ is imaginary so that y_m is hyperbolic sine function and so it grows up without constrains. At the boundary of this condition the resonator is conditionally stable because small errors in the alignment may render it unstable.
Until now we have talked about rays but it is possible to obtain similar result also for beams.
Inside a cavity a beam can exist consistently only if is radius of curvature of the wavefronts beams at the two mirrors coincide with the one of the mirror. In few words it can exist if and only if is a solution of the paraxial Helmholtz condition (Eq.2.1.0.2) and it satisfies the boundary conditions due to the mirrors.
Let's suppose to choose a coordinates system that has the position of the waist in the cavity at 0. We will define z_1 and z_2 respectively the position of M_1 and M_2 in this reference frame. If the length of the cavity is L then $z_2 = z_1 + L$. z_1 and z_2 are obtained matching the value of the radius of

curvature of the beam ($R(z) = z + z_0^2/z$) with the one of the mirror.
Starting from these hypothesis it is possible to calculate the values of z_1 and z_2:

$$z_1 = \frac{-L(\rho_2 + L)}{\rho_1 + \rho_1 + 2L} \tag{2.2.3.5}$$

and z_2 is immediately derivable from this. Also z_0 can be derived:

$$z_0^2 = \frac{-L(\rho_2 + L)(\rho_1 + L)(\rho_1 + \rho_1 + L)}{(\rho_1 + \rho_1 + 2L)^2} \tag{2.2.3.6}$$

z_0 should be real for guaranteeing that this is a gaussian beam but it means that $z_0^2 \geq 0$. Then it is easy to prove that:

$$0 \leq \left(1 + \frac{L}{\rho_1}\right)\left(1 + \frac{L}{\rho_2}\right) \leq 1 \tag{2.2.3.7}$$

which is exactly the same condition derived before with only rays.

2.2.4 Resonance condition

As said in the introduction of this section FPC are used as resonators. A basic version of a resonator is a system composed by two planar mirrors with no transmission, one in $z = 0$ and the other one in $z = L$.
It is known [7] that the wavefunction of a monochromatic wave of frequency ν is:

$$u(\vec{r}, t) = Re\{U(\vec{r})e^{i2\pi\nu t}\} \tag{2.2.4.1}$$

Where $U(\vec{r})$ is called complex amplitude and satifies the Helmholtz equation $\nabla^2 U + k^2 U = 0$ with $k = \frac{2\pi\nu}{c}$.
One of the solutions for this system is the one with $U(\vec{r}) = 0$ in $z = 0$ and in $z = L$. Consequently:

$$U(\vec{r}) = \sin(kz) \tag{2.2.4.2}$$

with k which satisfies the condition $kL = n\pi$ where n is an integer. From this last constrain the condition on allowed frequencies results is:

$$\nu_n = \frac{nc}{2L} \tag{2.2.4.3}$$

These frequencies are always separated by:

$$\nu_F = \frac{c}{2L} \tag{2.2.4.4}$$

Which coincide to the fundamental frequency of the resonator and with the FSR of the cavity.
In the case of beams, as said in (2.1.0.8), the phase factor is:

$$\phi(\rho, z) = kz + k\frac{\rho^2}{2R(z)} - \zeta(z) \tag{2.2.4.5}$$

The change of phase in a round trip is:

$$2(\phi(0, z_2) - \phi(0, z_1)) = 2kL - 2(\zeta(z_2) - \zeta(z_1)) \tag{2.2.4.6}$$

If it has to be a stationary wave this phase change has to be a multiple of 2π and so:

$$kL - (\zeta(z_2) - \zeta(z_1)) = n\pi \tag{2.2.4.7}$$

Consequently the allowed frequencies are:

$$\nu_n = n\nu_f + \frac{\Delta\zeta}{\pi}\nu_f \tag{2.2.4.8}$$

where ν_f is the fundamental frequency $\frac{c}{2L}$ and $\Delta\zeta = \zeta(z_2) - \zeta(z_1)$. As it is possible to see the result is completely similar to the previous one.

2.2.5 Misalignment effects

In order to know how much accurate it's necessary to be in the production and alignment it's important to understand how an axial displacement between the mirrors or an angle tilt of one of them change our cavity parameters. In this sense it's useful to give an estimation of the efficiency given by the coupling and we estimate it for a generic system composed by two optical devices. In our case it will be between an FPC and the fiber core.
The starting point is to consider a circular symmetry gaussian beam so without any different x-y confinement or astigmatism problems.
We can easily suppose that the total coupling efficiency will be defined by three different contributions [14]:

$$\epsilon(r, \theta) = \epsilon_0\tau(\theta)D(r) \tag{2.2.5.1}$$

where ϵ_0 is the coupling system between two optical system without any misalignment, $\tau(\theta)$ is the contribution of an angular tilt and $D(r)$ is the contribution of a displacement. Aim of this section is to derive all these contributions.
In order to calculate ϵ_0 we can imagine to write down the wave function after one of the devices in the x-axis as:

$$|W,\kappa\rangle = (2/\pi)^{1/4} W^{-1/2} e^{-(x/W)^2 + \frac{1}{2}ikx^2} \tag{2.2.5.2}$$

where W is the beam radius and κ is the curvature at z fixed.
The coupling efficiency is therefore given by the square module of the projection between the initial state to the final one:

$$\begin{aligned} \epsilon_{0x} &= |\left\langle \bar{W}, \bar{\kappa} | W, \kappa \right\rangle|^2 = \\ &= \frac{2}{((\bar{W}/W + W/\bar{W})^2 + (k\bar{W}W/2)^2(\bar{\kappa}-\kappa)^2)^{\frac{1}{2}}} \end{aligned} \tag{2.2.5.3}$$

This last equation is written in local representation but it is possible also to write it in terms of the waist sizes $\bar{W}_0$ and W_0 and the distances to the projection plains $\bar{z}$ and z as

$$\epsilon_{0x} = \frac{2}{((\bar{W}_0/W_0 + W_0/\bar{W}_0)^2 + (2/(k\bar{W}_0 W_0))^2 s^2)^{\frac{1}{2}}} \tag{2.2.5.4}$$

with $s = \bar{z} - z$. It is evident that this is only the contribution in one of the axis. The exact estimation is the square of it (it derives from the circular symmetry).
The contribution due to the angular tilt is obtained in a similar way. Indeed, with a small angle tilt, the wave function changes of an additional phase angle $k\theta x$:

$$|W,\kappa,\theta\rangle = (2/\pi)^{1/4} W^{-1/2} e^{-(x/W)^2 + i(\frac{1}{2}kx^2 + k\theta x)} \tag{2.2.5.5}$$

As before we will compute the coupling efficiency as the square module of a projection:

$$\tau(\theta) = |\left\langle \bar{W}, \bar{\kappa}, 0 | W, \kappa, \theta \right\rangle|^2 = \epsilon_{0x} e^{-(\theta/\theta_e)^2} \tag{2.2.5.6}$$

where θ_e can be defined as:

$$\theta_e = \frac{\sqrt[3]{2}}{k\epsilon_{0x}(\bar{W}^2 + W^2)^{1/2}} \tag{2.2.5.7}$$

As before, substituting to $\bar{W}$ and W their definition we can obtain this formula in term of the waist sizes and of the distances.
For the axial displacement the calculation is a limit case of the angular one. Indeed an offset is indistinguishable from a angular tilt of $\theta = d/z$ at $z \to \infty$. So as $z \to \infty$ we introduce $\theta = d/z$ and we substitute $\bar{W} \to 2\bar{z}/(k\bar{W}_0)$ and $W \to 2z/(kW_0)$:

$$D(d) = \epsilon_{0x} e^{-(d/d_e)^2} \tag{2.2.5.8}$$

where:

$$d_e = \frac{\sqrt{2}}{\epsilon_{0x}(1/\bar{W_0}^2 + 1/W_0^2)^{1/2}} \tag{2.2.5.9}$$

To sum up the total efficiency to couple from an optical device to second one will be in the end:

$$\epsilon(r, \theta) = \epsilon_0 e^{-(d/d_e)^2} e^{-(\theta/\theta_e)^2} \tag{2.2.5.10}$$

Chapter 3

Experimental part

3.1 Example of cavity characterization

In order to understand what are the interesting parameters in a cavity and their orders of magnitude may be useful to present the techniques to characterize and analyse a Fabry-Perot Cavity (FPC). Here below are shown the measurements done with two fiber mirrors produced at ESN in Paris and then used in the Cavity QED experiment group in Innsbruck.
In this section the techniques used will be presented and discussed. For doing this kind of measurement the setup normally used is shown in Figure 3.1
It is composed by a laser source (in our experiment with a wavelength of 844

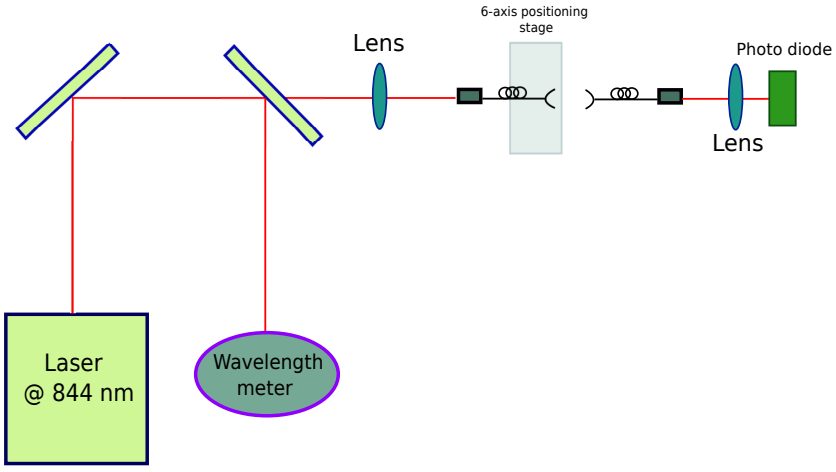

Figure 3.1: Cavity characterisation setup. A laser is coupled in the first fiber. The other tip is in front of a secondo fiber and with this it form a cavity. With a piezo controlled 6-axis stage it is possible to change the length of the cavity and with a photodiode transmitted light intensity can be measured

nm). The laser beam is immediately split: one part is sent to a wavelength meter and the other part is sent properly to the experiment. Here the beam is focused by a lens and then coupled into a single-mode fiber positioned inside an holder. The other tip, the one with the high-reflectivity mirror, is fixed to a 6-axis positioning stage which is moved by a piezoelectric actuator. The actuator is controlled by a standard function generator.
Then a multi-mode fiber with the mirror is mounted onto a fixed holder in front of the other one. In the end the beam outside this cavity is re-focused with another lens and its intensity is recorded by a photo-diode. The signal is displayed and saved with an oscilloscope.
The experimental procedure is composed by two main steps:

1) **FWHM measurement**
   The piezo actuator is turned on and controlled by the function generator with a sine shape at a frequency $f \approx 20$ Hz. Single mode fiber is now moved forward and backward with this frequency. Doing this the light inside the cavity is sometimes in resonance and sometimes not depending on the cavity length and the intensity change consequently. It's evident at this point that what we are looking at is the resonance frequency an so this is a frequency-domain measurement. Obtained and optimised the resonance peak it'll require calibration because until now no frequency reference is available.
   In order to calibrate the x-axis of the plot in term of frequencies it is

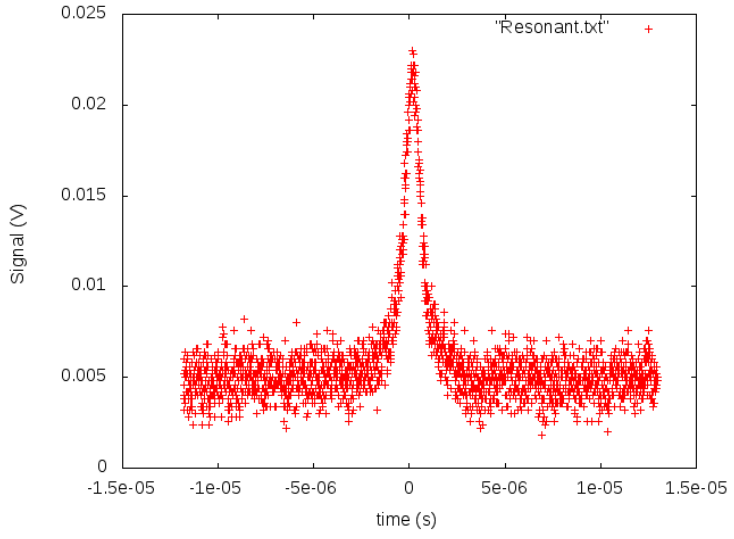

Figure 3.2: In orange an example of resonance spectrum from the oscilloscope

necessary to introduce some known reference on the axis. Therefore we

introduce a frequency modulation on the laser beam with a Marconi generator (at $\approx$ 100 MHz). It is possible to prove that the expected signal from that is mainly composed by three peaks, a central one, corrisponding to the previous peak, which is higher and two side ones, called the sidebands, distant from the first the modulation frequency.

With this method we cannot estimate the exact frequency of the

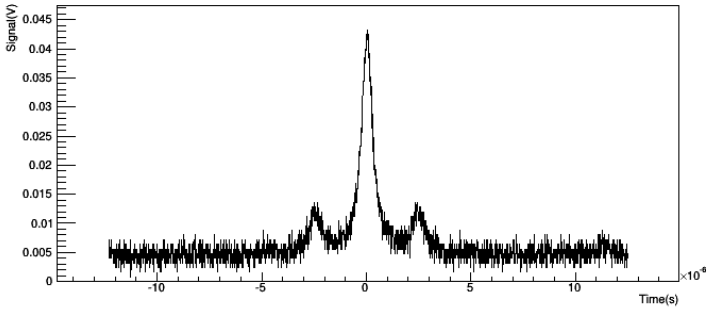

Figure 3.3: Spectrum acquired from the oscilloscope with the modulation. In this plot two sidebands are visible on the sides of the central peak.

peak but we need to know in frequencies terms the FWHM and so this differential measurement is sufficient.

2) Measurement of the FSR

The free spectrum range is the separation between two longitudinal modes. In order to calculate it is necessary to measure the cavity length which is possible to derive it when different resonant wavelengths are known. This is done by changing the wavelength of the laser and modifying the grating angle, looking for resonances through the oscilloscope. The measurement is performed with the wavelength meter.

Another method, which is used only in particular circumstances, is to acquired a spectrum with two resonant peaks and calculate their distance.

The main parameter that we want to estimate is the FWHM and the FSR. It is possible to obtain it simply with a proper fit. From some frequency spectra is evident that the resonance peaks are really far between them and so a linear approximation is acceptable. The distribution in this terms is a Loretzian one.

So we will fit the data with the sum of three Lorentzian distributions, one

for peak:

$$f(x) = A_1 \frac{\sigma_1}{(x-x_1)^2+\sigma_1^2} + A_2 \frac{\sigma_2}{(x-x_2)^2+\sigma_2^2} + A_3 \frac{\sigma_3}{(x-x_3)^2+\sigma_3^2} + B \tag{3.1.0.1}$$

where A_i is the normalization constant of the i−th Lorentzian distribution, x_i the position of the peak and σ_i its Half Width Half Maximum (HWHM) with $i = 1, 2, 3$ corrisponding on the i-th peak. B is added for taking into account the presence of a constant background.
We have obtained from the fit the following results:

Parameter	Value
A_1	$2.30 \pm 0.06 nsV$
x_1	$-2.44 \pm 0.01 \mu s$
σ_1	$0.3521 \pm 0.0003 \mu s$

Parameter	Value
A_2	$11.48 \pm 0.09 nsV$
x_2	$0.00035 \pm 0.00002 \mu s$
σ_2	$0.307 \pm 0.003 \mu s$

Parameter	Value
A_3	$2.23 \pm 0.06 nsV$
x_3	$2.50 \pm 0.01 \mu s$
σ_3	$3.377 \pm 0.004 \mu s$

The reduced χ^2 of the fit is equal to 0.004 and the plotted obtained function is shown in Figure 3.4. The estimated constant background is $B = 4.65 \pm 0.03$ mV.
From the FSR measurement it has been obtained different wavelengths and calculating the cavity length as $L = \frac{\lambda_1 \lambda_2}{2(\lambda_2 - \lambda_1)}$ and then doing the mean, $L = 89 \pm 10 \mu m$ where the error is calculated as the standard deviation of multiple measurement. The Free Spectral Range is calculated as in (2.2.2.1), FSR = c/2L $= 1.6 \pm o.2$ THz.
Now, let's characterise the cavity from these raw parameters.

First of all it's necessary to calibrate the spectrum. It's evident that the FWHM in the frequency domain can be derived from the proportion:

$$2\sigma_2/(x_1 - x_3) = FWHM(Hz)/200MHz \tag{3.1.0.2}$$

And then:

$$FWHM(Hz) = \sigma_2 400MHz/(x_1 - x_3) \tag{3.1.0.3}$$

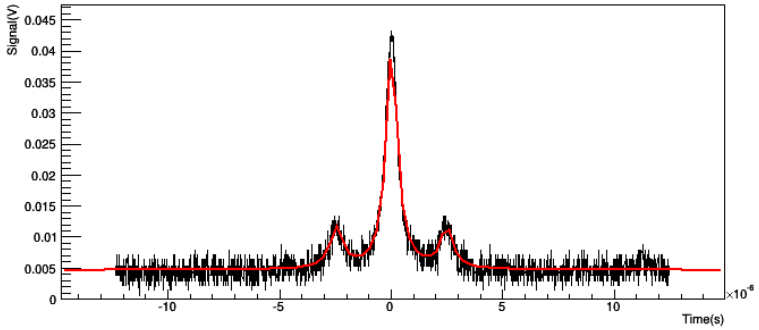

Figure 3.4: Fitted spectrum. In this plot are shown both the fitted function and the data. x_1, x_2 and x_3 labels the peaks

We know that F = FSR/FWHM and so we obtain:

$$FWHM = 249.0 \pm 0.4 MHz \tag{3.1.0.4}$$

$$F = (67 \pm 7) \cdot 10^3 \tag{3.1.0.5}$$

where the error is obtained by propagation from the fit errors.

3.2 Setup

The idea, as explained in the introduction is to implement a setup for mechanically produce fiber tips. The setup geometry is quiet similar to the one used in Glessen group at Stuttgart but adapted for standard silica glass and with different improvement. In this section the experimental setup will be presented part by part.

As shown in Figure 3.5 our experiment is composed by many stages but its core is mainly done with an heater (1), an holder for the spheres and movable support for the fiber (respectively 3 and 2).

The experiment is built on an breadboard mounted into a vertical position on a standard optical table. We have tried to mount the experiment in vertical and in horizontal but the first alternative is the best because it allows to use a constantly pressing stage for the force sensor, as it will be better explained in Section 3.2.4.

The sphere holder is composed by a metallic cylindrical support that keep fixed a small ceramic pipe with two small rubber band and an holed metal tube of the same dimension. This holder is connected to a mechanical vacuum pump (7) which keeps hanging the sphere by suction.

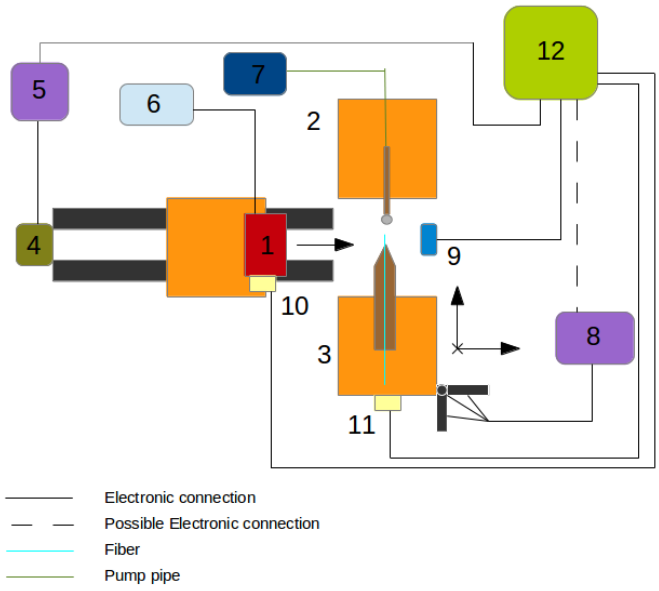

Figure 3.5: Experiment scheme

The heater is mounted on a rail and moved by hand but in the future we will implement automatic movement done with a stepper motor (4) on a linear rail. The stepper motor is supplied by a driver (5) connected to an Arduino Board that give the timing for controlling the movement. The heater is powered with an external high power supplier.
The fiber is kept static inside two ceramic plate with a V-groove and moved with motorized stages in all the possible direction for having the possibility to well align the fiber and the spheres center.
The measurements are done by a thermocouple type R (10) or by a thermocamera and a force sensor (11) and their signals are read through the Arduino board after a proper electronic chain. (6) and (8) are the power supply for the heater and the motorized stage of the fiber holder. The complete experiment is managed by a GUI on a computer (12) programmed with C++ and QT libraries which store the data from the sensor and at a later time also the experiment movement.
Two digital microscopes (9) have been mounted in two orthogonal direction in order to have 2 optical access when the heater is not on the holders. These are used for the complete centering. When the heater is moved on the fiber-sphere system only one of these microscope is used as feedback for the

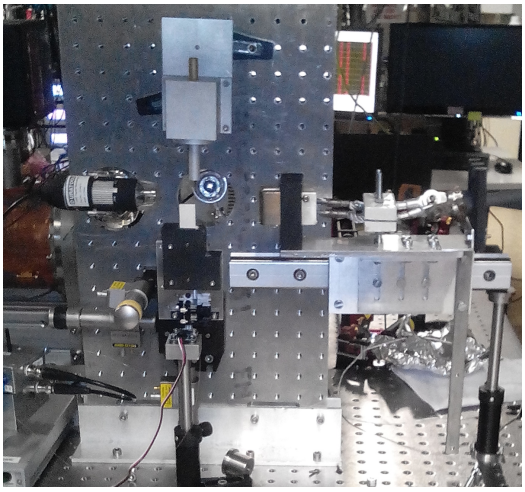

Figure 3.6: Photo of the complete experiment. On the right there is the heater mounted on its rail, At the bottom the fiber holder with the mounting for the force sensor. On the top there is the fixed sphere holder. In the hole in the center and on the left are mounted the digital microscope.

process.

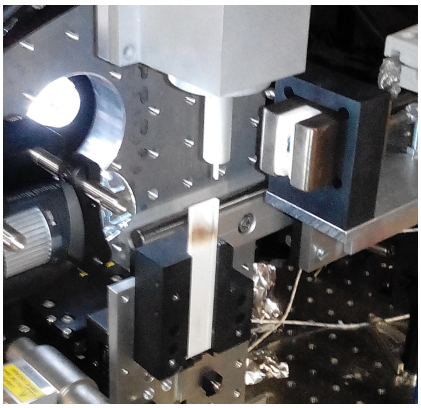

Figure 3.7: Image of the core of the experimental setup.

All these parts will be shown in details in the next sections.

3.2.1 Fibers

The fibers used in the experiment are of two cladding diameter (125 or 200 μm) and they can be single-mode or graded index multi-mode. It is of interest produce concave end-face with both the typologies.

The fibers are composed by multiple layers with different functions. They are from the outside to the inside:

- A copper coating which is used to avoid to break the fiber if bent. In any case, copper is one of the few material which is vacuum compatible (we need to integrate this fiber in a CQED experimental setup in ultra high vacuum).
- A titanium/carbon coating which adds more resistance to the bending and is used in particular as an adhesive layer between the glass and the copper.
- The cladding which is a portion of the fiber which is in silica glass.
- The core is a small portion of the fiber in silica glass with different composition from the cladding where the light passes. In order to guarantee light confinement it has a different refractive index. If the fiber single-mode it will have a diameter of $\sim$ 6-10 μm otherwise it will be of $\sim$ 50-60 μm

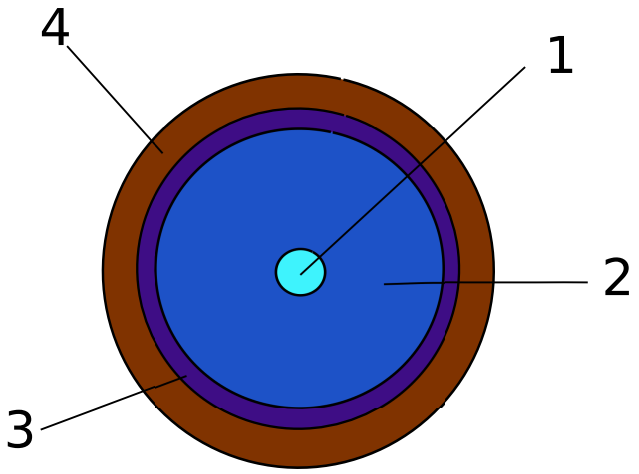

Figure 3.8: Fiber structure: the outer layer (3) is the copper coating then there is the titanium one and the cladding and the core (2 and 1)

The fibers used in the experiment are described in the table below[1]

[1]http://www.ivgfiber.com/

	Single-mode	Multi-mode
Coating material	Copper	Copper
Inner coating	No	Yes
Wavelength	800-900 nm	600 - 2000 nm
Attenuation at 800 nm	10.5 dB/km	14 dB/km
Numerical aperture	0.13	0.22
Core/clad composition	Ge-Doped/pure	Ge-Doped/pure
Cladding diameter	125 ± 1 μm	200 ± 2 μm
Coating diameter	165 ± 10 μm	260 ± 10 μm

3.2.2 Spheres

The spheres on the other hand should resist to high temperature and to high thermal stresses. They have also to have a low roughness ($\approx$ 10 nm) so that, after having produce the fiber tips, the profile produced should be simpler to smooth it with a laser. Here below a table with the chosen materials and their main properties[2]:

	Sapphire	Rubin	Silicon Carbide
Chemical Formula	Al_2O_3	Al_2O_3/Cr_2O_3	SiC
Diameter (mm)	0.5	0.5	0.5/1.75
Specific heat (J/kgK)	755	755	600
Density (g/cm^3)	3.99	3.99	3.15
Thermal conductivity (W/mK)	36	36	100
Melting Point	$1800°C$	$1800°C$	$1500°C$

All these materials have been tested and they are compatible with the fiber. Indeed the fibers doesn't remain glued to the sphere in the interesting temperature range. Fibers continue to transmit light and so there are no despicable change in interesting optical properties has been seen.

3.2.3 Heater

In this experiment it is necessary an high temperature source and different solutions are possible. The request are:

- it is heated up between $1200°C$ and $1600°C$ (Melting temperature of the silica glass) with variable temperature in this range.

- it should involve a volume as small as possible.

[2]http://www.saphirwerk.com/english/

- it has to work in air and so it hasn't to have any oxidation problem in that range

- it should be possible to move back the heater or to turn off/on it fastly so that it hasn't to be necessary to wait to much time in order to cool down the fibers.

In order to do that we used an heating element by Kanthal in molybdenum disilicide ($MoSi_2$). It is a resistive part that has a custom shape made like in Figure 3.9. This material may heat until $1850°C$.
It is the only electrical solution that is guaranteeing a stable full control on the temperature due to the power used.

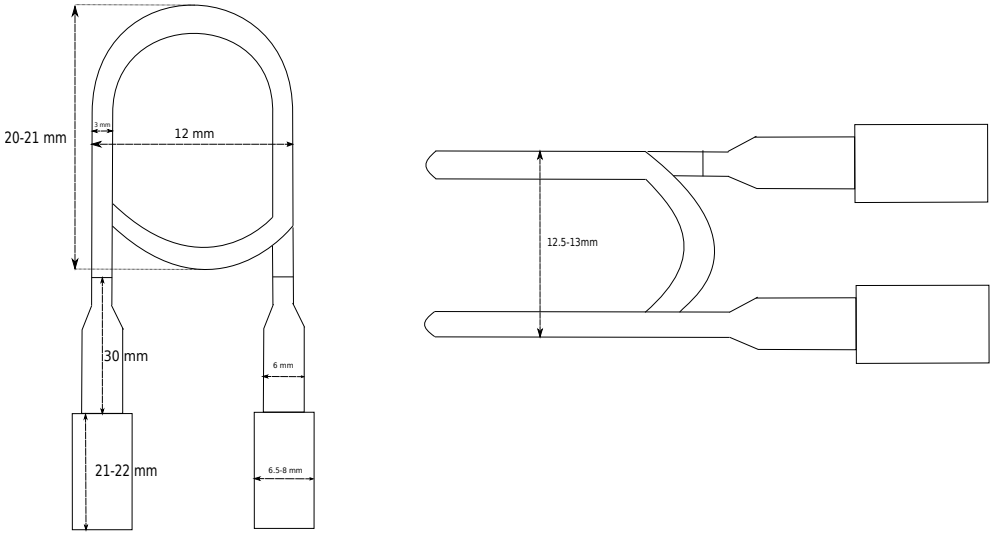

Figure 3.9: Scheme of the heating element

In order to improve the performances of the heater it's necessary to confine the heat and doing it is simple with a furnace in ceramic. In the experiment it has been used a custom one (see Figure 3.10). It has this C-shape in order to guarantee to cover completely the fiber-sphere system and to be removable.
For safety questions it's necessary to separate the wires in which high current flows and for that we used two support, one in ceramic near the ending of the furnace and another one in plastic.
The heater is supplied by a maximum power of 350 W.
For the movement a custom made slider has been used. It is done with some internal bearings for reducing the friction and it is moved manually as shown in Figure 3.11.

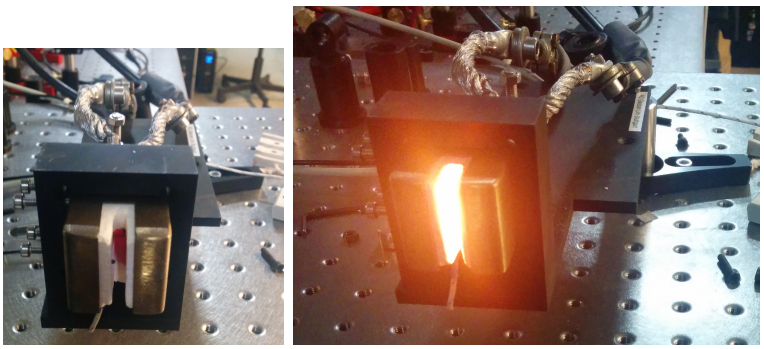

Figure 3.10: Images of the heater. A metal holder keeps fixed a ceramic oven. The heating element is situated inside this. The two photos show the heater with different power supplied.

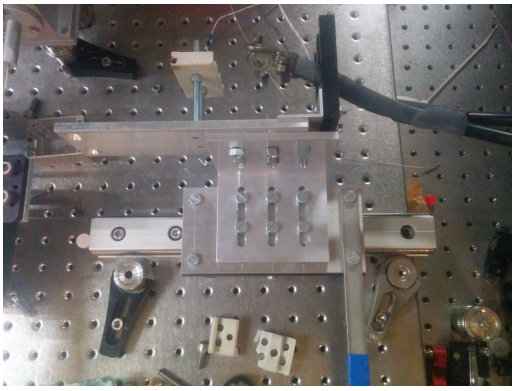

Figure 3.11: Photo of the slider used in the experiment. No automatic movement has been implemented yet and this is moved manually with n handle.

3.2.4 Sphere and fiber holder

It's evidently necessary to have an holder either for the sphere and for the fibers to allow correct and reproducible movements.
For the fibers an adapter to the optical table is needed. The holder is built in aluminium and the parts in contact with the heater in glass ceramic. In particular this last part will be composed by two pieces of ceramic with a V-groove hole with a diameter of $\sim 200\ \mu m$ in the middle. A good alternative that avoids any ceramic machining is to use a ceramic tube and fix and align it with standard opto-mechanical equipment. During the experiment we tested both.

For the spheres we used directly a ceramic tube insert inside an holed

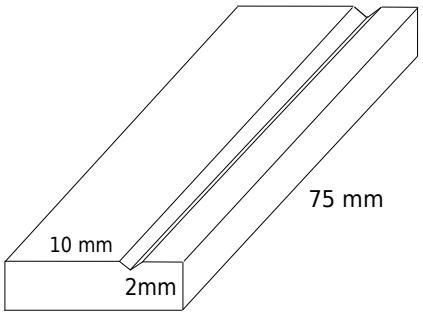

Figure 3.12: Axonometric projection of one of the two mirrored parts that composed the fiber holder. The two parts leave a rotated square-shaped hole

aluminium cylinder. The static positioning it is guaranteed by a proper mounting composed by a first rubber band, a small metal tube and another rubber band as shown in Figure 3.13. All these parts are fixed with an holed screw and mounted onto the optical breadboard trough an adapter. This is then connected to a mechanical vacuum pump that block the sphere to the end face of the ceramic tube by suction.

It's necessary in both the holders that the aluminium parts doesn't touch the heater and so the ceramic parts have to have a proper length.

Also the selection of the ceramic for this holder has to be appropriate but this will be discuss in the Section 3.3.4.

3.2.5 Force sensor

In order to get reproducible fiber, it's necessary to know how much is the force applied by the fibers on the spheres. It can be also useful to have a feedback to know the exact moment when fiber and sphere are in contact. Indeed the light from the heater is so bright to blind the microscope. It can

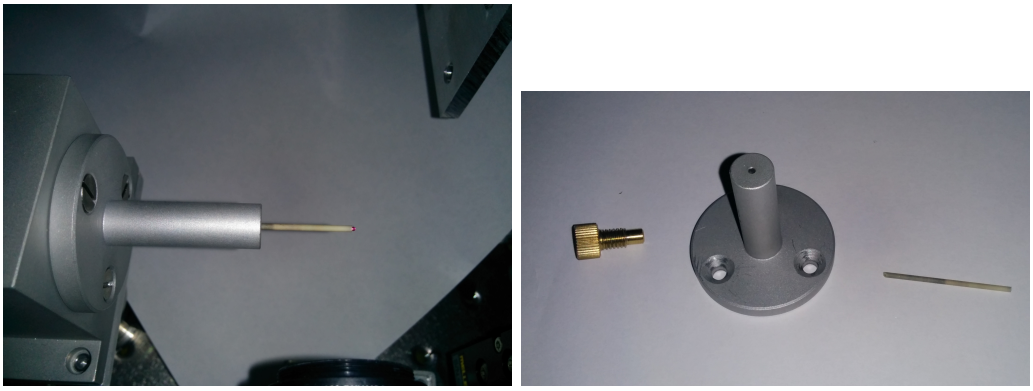

Figure 3.13: Photo of the sphere holder (on the left) and of its mounting (on the right)

be prevented by adding an absorptive filter.
The best way for having this force feedback is to do a direct force measurement. In this experiment it is used the force sensor in Figure 3.14 (Thin force sensor 1130 by Phidgets) because its size fits well with the experimental setup and for that easily integrable in the holder.

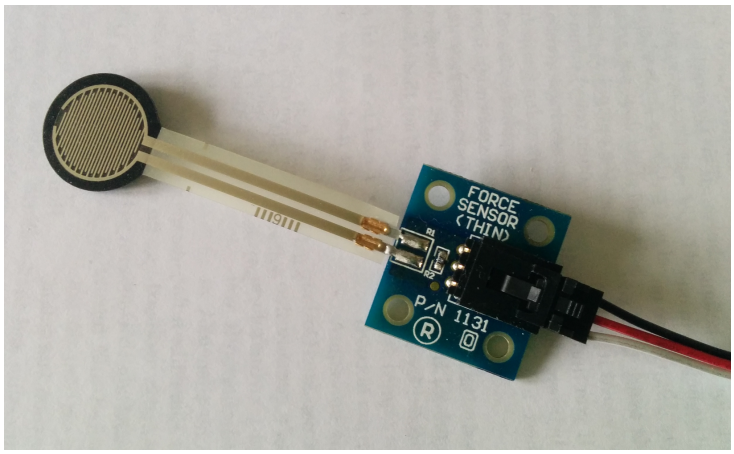

Figure 3.14: The force sensor used in the experiment

The properties of this sensor are listed in the table below [3]

[3]http://www.phidgets.com/

Force Min	1 N
Force Max	20 N
Max Measurement Error	10%
Working temperature range	Between $-30°C$ and $70°C$
Supply voltage range	Between 4.5 to 5 V DC

It's necessary to do reproduce the measurement and so we choose to position the force sensor on the bottom of a stage where is mounted the fiber holder. The stage has been modified removing the springs. The breadboard where the experiment is built, is in a vertical position and in this way the movable part of the stage always compresses the force sensor and, properly calibrating, it's possible always to do a differential measurement and so to know how much is the force applied on the sphere.
For our purpose it's necessary to optimize the signal and to have some system to store this data. In term of signal it's necessary to erase the offset due to the constant weight of the stage and then to amplify it in order to optimize it and to allow a better data acquisition with an Arduino board.
We have also seen that the signal from the sensor has an offset of $\sim 3V$ and

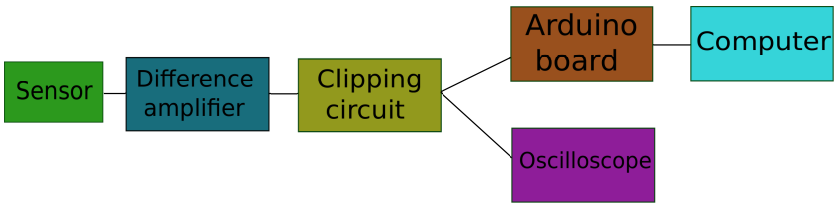

Figure 3.15: Scheme of the electronic chain for the force sensor

a useful range of $\sim 0.5V$. For this reason it has been projected and built the electronic circuit in Figure 3.16.
It is composed by three parts (one for every operational amplifiers). The first part is a buffer necessary to produce the an uncoupled offset constant signal. This signal can be changed changing the resistance value on the resistor. It is also possible with a switch to insert an offset through an external source instead of the internal one (particular useful in the case of variable offsets).
The second is a difference amplifier with unitary gain that subtracts the offset from the sensor signal. In order to build a very accurate device which perform only the difference between the signals in this part it has been used very accurate resistances which does not differs more $\Delta R < 0.1\%$ one from another.
The last part is a non-inverting amplifier with a variable amplification.
In the lab different sources of noise have been seen. For example the ion traps of the other experiments are known sources of radio frequency signal

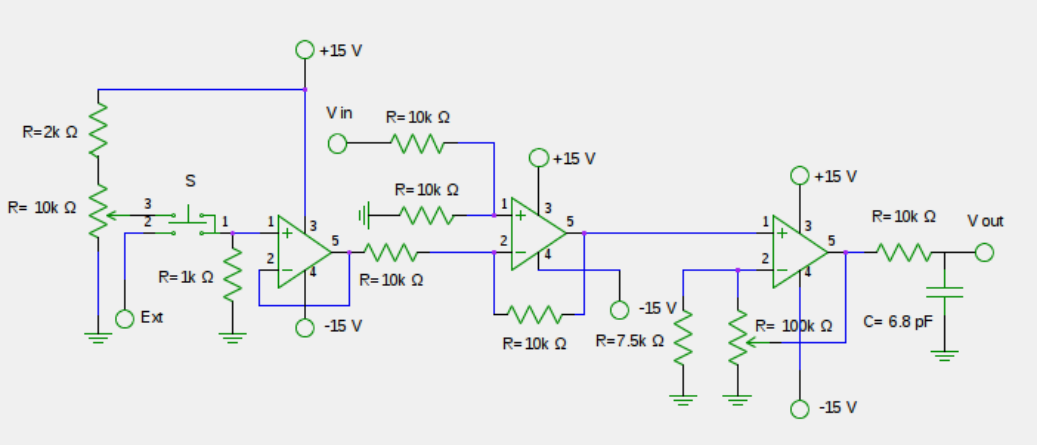

Figure 3.16: Difference amplifier for the force sensor. With this circuit it is possible to remove a variable offset using as reference the voltage supply for the operational amplifiers or using an external source. Then it is possible also to amplify.

that may cause misleading measurements. So it has been necessary to filter the high frequencies with a simple low pass filter and to cage it in a metal box. The circuit is powered by an external power source.
All the characteristic parameter of the circuit has been listed in the following table:

Voltage supply	$\pm 15V$
Amplification	From 1x to 15x
Bandwidth (1x Amp)	(150.0 ± 1.6) kHz
Inner offset range (1x Amp)	from 0 V to -3.72 V

Modifying the amplification of the circuit may be misleading if it's necessary to digitally convert it an may cause damage to the converter. Indeed Arduino board cannot correctly convert over 5 V and the working threshold is 5.5 V. For avoid overvoltage and voltage peaks so it is also necessary to use a clipping circuit that let it pass the signal only if it is less than a defined threshold otherwise the signal is saturated to the threshold value respectively.

At the end of this electronic chain there is an Arduino Uno board that digitally converts the signal and sends this data to the computer. Arduino Uno ADC has 1024 bit of resolution and so it can read until $\approx 5mV$. The board has been programmed so that is it possible to change also the time sampling from $10\mu s$ to $1s$. The PC manage the data with the GUI previously mentioned.

We also noticed a drift in the signal which can introduce a bias error (also

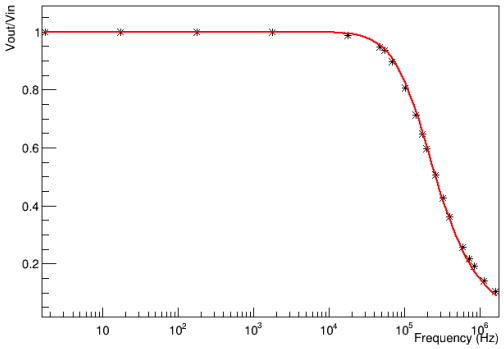

Figure 3.17: Frequency response of the circuit at 1x Amp. This measurement has been done using as input a sine signal with fixed amplitude. It consists in changing frequency and looking at the output amplitude

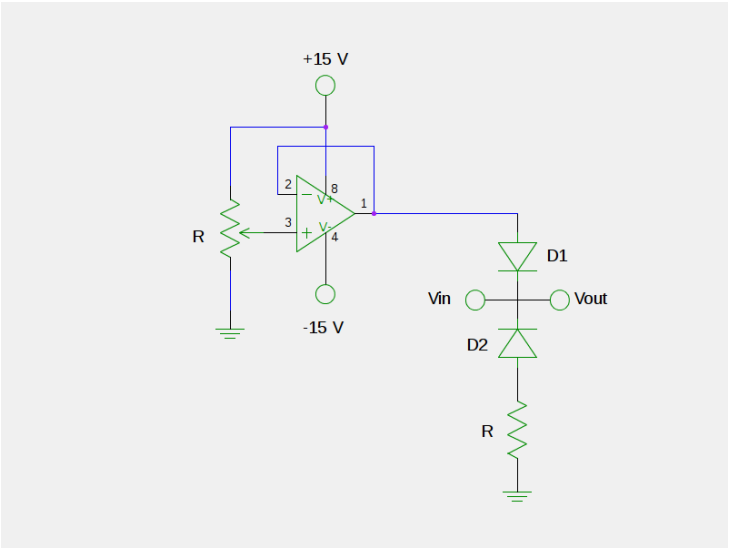

Figure 3.18: Clipping circuit for the force sensor

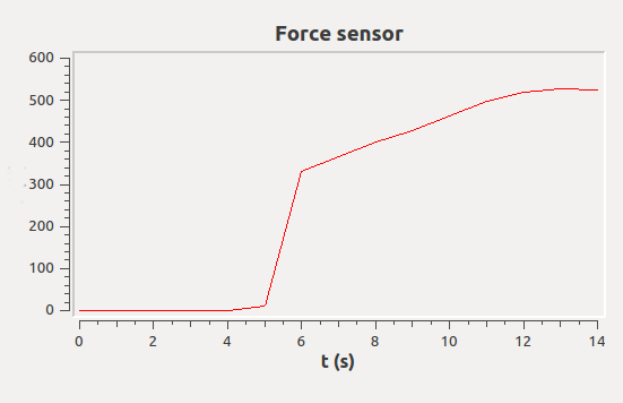

Figure 3.19: Example of the output from the GUI for force data. In this case th sampling time has been set to 1 s and the signal isn't modified calibrated yet.

provided by the datasheet). It begins to be relevant after $\tau \sim 1hr$ of usage which is the timescale for producing a fiber. In order to solve this problem, it is possible to carry out a very fast calibration procedure every time that this sensor is exploited and it guarantees reproducible measurement.
The calibration curve is not linear, in particular it is suggested by the force sensor datasheet report:

$$F(N) = Ae^{Bx} + C$$

where x is the signal acquired from the arduino board and A, B, C are parameter to determine with a fit.
To sum up in Figure 3.15 the complete electronic chain of the experiment with every connection.

3.2.6 Temperature measurement

There are different possibilities for measure the temperature in our experiment. The easiest way to do it is to use thermocouple positioned inside the heater. Because of the temperature range involved in the process the best choice is a thermocouple of type R that has a maximum measurement threshold at about $1600°C$. This kind of sensor however:

- has a not properly linear response in term of electric signal to very high temperature;
- measures the temperature in the point in the furnace in which it is put and not in general on the fiber tip or on the heating element. It's not

correct to assume the homogeneity of the temperature in the heater and so this measurement isn't really useful in term of reproducibility because this information cannot be used in different kind or geometry of furnace.

- requires a calibration and this means that some references are needed at very high temperature.

Another possible choice should be a thermocamera which use the emitted light by the heating element (and so give us the exact temperature on the heater). The one we used had a very large range (). We have done some calibration measurement in order to understand the correlation between the electrical power that supplies the heater and the temperature.

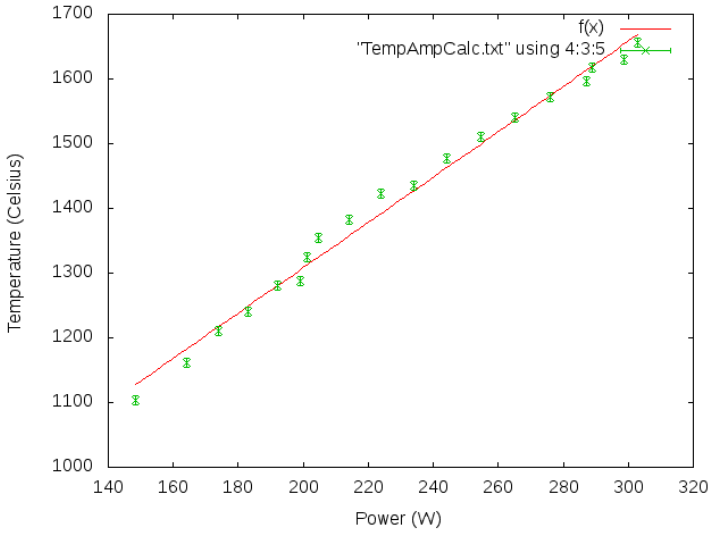

Figure 3.20: Calibration curve. It is shown a linear dependency between the power which supplies the heater and the measured temperature. In the temperature between $1300°C$ and $1450°C$ this instrument has an evident thermal drift.

It has been done a linear fit (f(x) = mx+q) and the obtained the results are:

$$m = 3.50 \pm 0.09°C/W \tag{3.2.6.1}$$

$$q = 608 \pm 20°C \tag{3.2.6.2}$$

Below the test of the residual is presented.

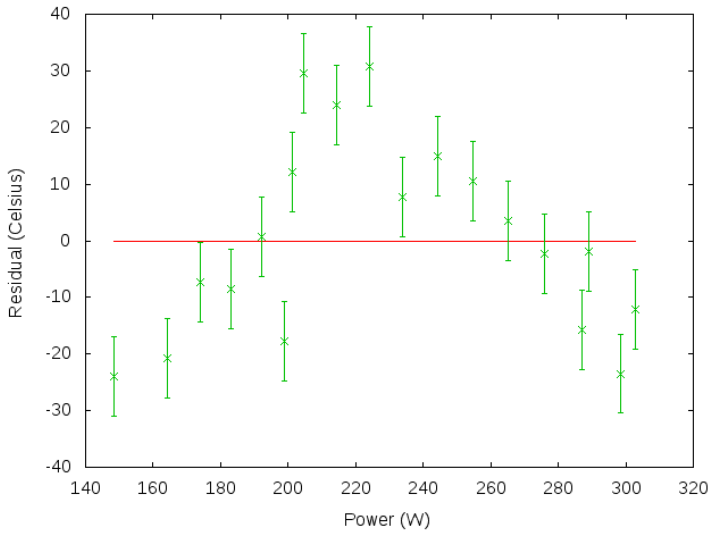

Figure 3.21: Residual of the calibration curves, The distribution of the points suggested that a linear assumption is good only in first approximation.

As it is possible to see from Figure 3.21 the data residuals are distributed in a very systematic way. This suggests us that the causes may be due to strong deviations from the linear behaviour or some thermal drift and probably a simulation is needed. Indeed, the relation between the electrical input power and the temperature of the heater will depends strongly depends on the geometry of the system and not all the power supplied is converted into heat. In any case few temperature are really useful in the experiment and for that we have some measurement reference.

3.3 The experiment

3.3.1 Simulation of cavity displacement

In order to understand the accuracy needed for producing fiber, a simulation was performed.
Although the presence of a displacement error between the fiber core and the central position on the mirror is probable, it is possible intuitively understand also that it is possible to partially compensate this error changing the relative positions of the mirror of the cavity and so the optical axis.
The model allows us to compute the total coupling efficiency between two spherical mirrors taking into account of the displacement error of the core of the fiber and of a displacement of the mirrors.

To implement this model it is necessary to known that optical axis is the line which pass through the center of sphere defining the mirrors [10].
Let's suppose to have composed by:

- A spherical mirror is at the end of the multi-mode fiber. It has the central position of the mirror at the origin of the axis and radius of curvature R_{MM}. The center of the spherical is consequently at $(R_{MM}, 0)$
- A spherical mirror is at the end of a single-mode fiber in front of the other one. It's radius of curvature is R_{SM} and the mirror central position is positioned in (L, y_0). The core of the fiber have a generic displacement d and the center of the spherical shape is at $(L-R_{SM}, y_0)$.

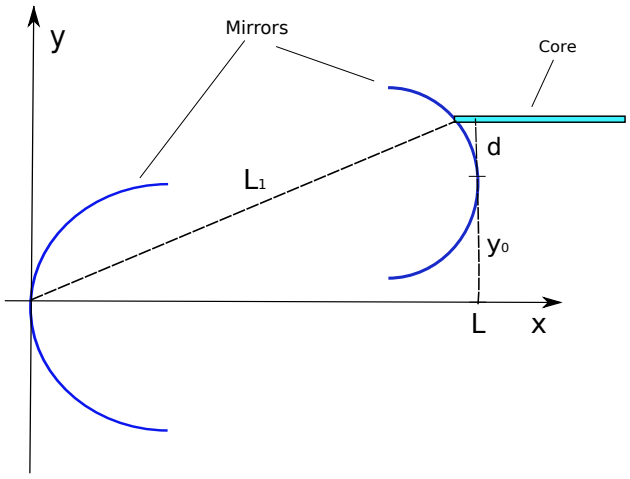

Figure 3.22: Scheme of the geometry of the cavities in the simulation. Even if the real system is three-dimensional the symmetry along the optical axis allow to study only it's planar projection

We can study this system using a simple bidimensional geometrical model because the system has a rotational symmetry along the optical axis [14].
It is possible to describe the mirrors as the circles of equations:

$$\begin{aligned} (x - R_{MM})^2 + y^2 &= R_{MM}^2 \\ (x - L + R_{SM})^2 + (y - y_0)^2 &= R_{SM}^2 \end{aligned} \tag{3.3.1.1}$$

Substituting in the equation we obtain that the fiber core will be at the coordinates $(L - R_{SM} + \sqrt{R_{SM}^2 + d^2}, y_0 + d)$. The line which connects the two centers is:

$$y = \frac{y_0}{L - R_{SM} - R_{MM}}(x - R_{MM}) \tag{3.3.1.2}$$

The length of the cavity will be defined by the intersection of the optical axis with the two mirrors and we obtain:

$$\begin{aligned} x_S &= L - R_{SM} + R_{SM}\sqrt{\frac{(L - R_{MM} - R_{SM})^2}{(L - R_{MM} - R_{SM})^2 + y_0^2}} \\ y_S &= \frac{y_0}{L - R_{SM} - R_{MM}}(x_S - R_{MM}) \\ x_M &= R_{MM} - R_{MM}\sqrt{\frac{(L - R_{MM} - R_{SM})^2}{(L - R_{MM} - R_{SM})^2 + y_0^2}} \\ y_M &= \frac{y_0}{L - R_{SM} - R_{MM}}(x_M - R_{MM}) \end{aligned} \tag{3.3.1.3}$$

The length of the cavity we obtain in this way will be:

$$L_1 = \sqrt{\left(\frac{y_0}{L - R_{SM} - R_{MM}}\right)^2 (x_S - x_M)^2 + (x_S - x_M)^2} \tag{3.3.1.4}$$

As seen in (name of the formula), it is necessary to know how much is the distance between the core and the optical axis and the angle between the core and the optical axis. Using some geometry formulas we obtain:

$$\begin{aligned} \Delta\phi &= \arctan\frac{y_0}{L - R_{SM} - R_{MM}} \\ \Delta d &= \frac{(L - R_{MM} - R_{SM})^2 d - y_0\sqrt{R_{SM}^2 + d^2}}{\sqrt{(L - R_{MM} - R_{SM})^2 + y_0^2}} \end{aligned} \tag{3.3.1.5}$$

Now we have defined all the geometrical elements for the simulation. We need for concluding to know some basic knowledges and assumptions about the beams after a fiber.
Indeed we assumed that the waist size inside a cavity can be rewritten in term of the stability factor g_1 and g_2 as:

$$W_0^2 = L\frac{\lambda}{\pi}\sqrt{\frac{g_1 g_2(1 - g_1 g_2)}{(g_1 + g_2 - 2g_1 g_2)^2}} \tag{3.3.1.6}$$

And that we can suppose that the waist size after a single-mode fiber should be the dimension of the core ($\sim 6\mu m$). In the same way it's possible to write down the focus depth as:

$$z_f = \pi\frac{D_{SM}^2}{\lambda} \tag{3.3.1.7}$$

$$z_c = \pi \frac{W_0^2}{\lambda} \tag{3.3.1.8}$$

where D_{SM} is the core diameter of the single mode fiber.
At this point we can calculate the total incoupling and using formulas (2.2.5.4), (2.2.5.9) and (2.2.5.7) we obtain:

$$\epsilon_0 = \frac{4}{(D_{SM}/W_0 + W_0/D_{SM})^2 + s^2/(z_f z_c)} \tag{3.3.1.9}$$

$$d_e = \frac{\sqrt{2}}{\epsilon_0 \sqrt{W_0^{-2} + D_{SM}^{-2}}} \tag{3.3.1.10}$$

$$\theta_e = \frac{\sqrt{2}}{\pi \epsilon_0 \sqrt{\left(\frac{W_0}{\lambda}\right)^2 + \left(\frac{D_{SM}}{2\lambda}\right)^2}} \tag{3.3.1.11}$$

where D_{SM} is the diameter of the core of the single mode fiber and s is the difference of the waist positions between the mode from the fiber and the one from the cavity.
So the coupling distribution derives from a modification of Equation (2.2.5.10):

$$\epsilon = \epsilon_0 e^{-(\frac{d-\Delta d}{d_e})^2} e^{-(\frac{\Delta\theta}{\theta_e})^2} \tag{3.3.1.12}$$

The coupling distribution changes if the parameters L and d are modified. Mainly three interesting results have being obtained from that:

- **Other stable positions**

It's well known that a stable position in an ideal cavity is the one with aligned optical axis. If the core of the fiber and the center of the mirror aren't overlapped, it may exist other well coupled positions where the optical axis of the two mirrors is not the same anymore.
The simulation suggested that this is not the case. Indeed with the simulation, fixing a value for the radius of curvature of the mirrors and of the cavity length, it is possible to see how the maximum coupling changes if the position of the second mirror is modified. In Figure 3.11 it is shown the result and as it is possible to see, the maximum is at the center.
A change in the position may improve the displacement contribution but the angle one may decrease and conversely.
It has been seen another interesting effect. Indeed changing the position of one of the mirrors shows a different position for the coupling peak. An example of this is shown in Figure 3.24.

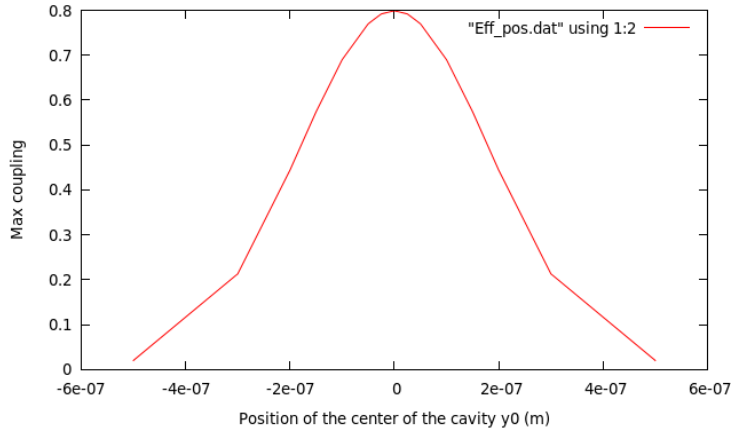

Figure 3.23: Plot of the maximal value of the coupling changing the position of one of the mirrors. The best position is with the two mirrors aligned with coincident axis.

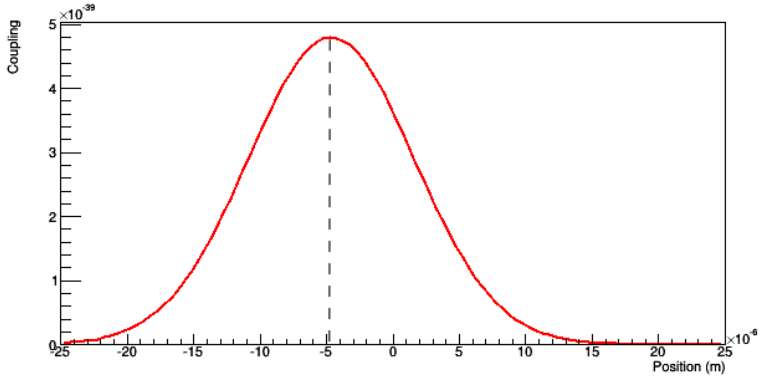

Figure 3.24: In this plot it is possible to see that to extreme movement of the mirror center corresponds a translation of the maximum in the coupling curve. This means on the other hand that exists position in which cavity is stable but not with good result in terms of coupling

- **Estimation of the accuracy in the process**

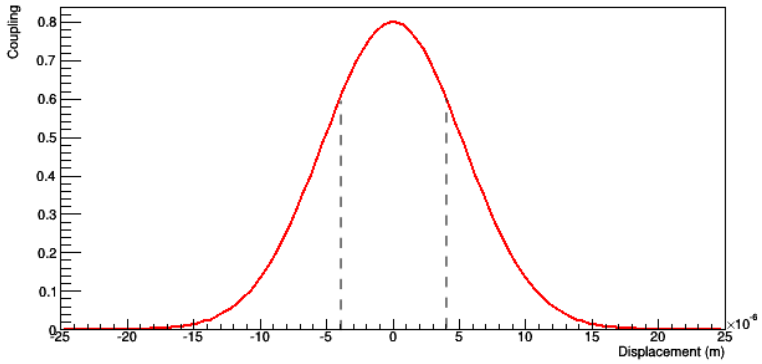

Figure 3.25: In this figure an estimation of the accuracy in the centering. It has to be of $\approx 4\mu m$ to reach a 60% coupling efficiency

Now it is well known that the best coupled cavity is the one with overlapped optical axis. Now it's immediate to calculate the accuracy assuming a given value of confidence. By fixing an acceptance threshold of coupling equal to 60% an accuracy in the alignment of $\approx 4\mu m$ is estimated (See Figure 3.25).

- **Optimal cavity length and mirrors radius of curvature**

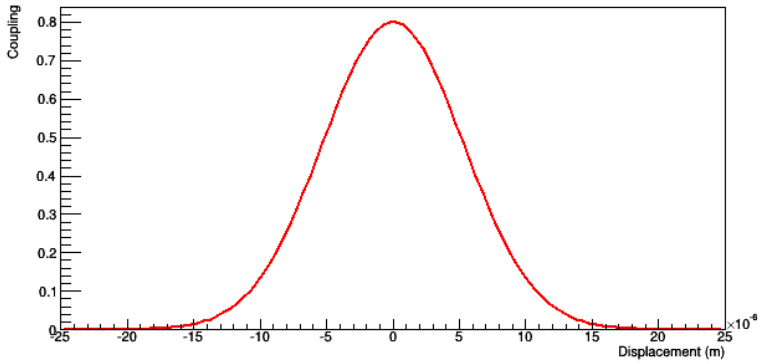

Figure 3.26: Here the final plot that optimize the coupling between the two mirrors. The radius of curvature are 500 μm and 750μm and for a distance of 200 μm give a coupling of 80%

The cavity length strongly influence the beam confinement. In our case we have a minimum length for the cavity that we wants to reach imposed by the

ion trap design.
Different configuration are acceptable, one of these can be with $R_{SM} = 500\mu m$ and $R_{MM} = 750\mu m$ with a cavity length $L = 200\mu m$. With these parameter the coupling efficiency is around 80%.
With this parameters set, the accuracy in the process should be of 4 μm in any case. An extended discussion on the techniques used in the experiment for centering the fiber and the sphere in order to obtain higher coupling will be presented in the next sections.

3.3.2 Experimental procedure

The setup and the following experimental procedure aim to reach these goals:

- Give a proof of principle that with this setup is possible to produce really concave spherical tips with a larger useful diameter (and so more stable and large cavities);
- To have the smallest roughness achievable;
- Automation in the process (Every action in the experiment should be easily verifiable);
- High reproducibility;
- To be cheap.

The reproducibility is a main topic in this experiment and it is assured by:

- The possibility to reproduce the initial condition before the experiment (Example: Temperature of the heater, alignment between the fiber and the sphere);
- Automatic movement (For the heater and for the fiber holder);

In this sense we already implemented every control for the initial condition. We have a centering procedure with good performances and we have checked the temperature stability of the heater.
On the other hand automation hasn't been implemented yet but during the build up of the experiment the apparatus was designed to host it (See for example the linear rail for the heater or the motorized stages for the fiber holder). In any case a program for manage all the movement and a project with a stepper motor for the heater has been already done.
The procedure will involve the following steps:

- Preparation of the experiment. This involve the cleaving and preparation of the fibers and the heating up of the heater;
- Check the quality of the cleaving through an optical microscope. It's important to see that the tip has no visible damage;
- Mounting of the fiber and of the sphere and centering;
- Production of the concave fiber tip. This will be deepened in the next sections;
- Check the differences in the fibers after the procedure with the optical microscope;
- Storing the fibers and do some profile measurement.

We need also to have a way in which is possible to clean the fiber tips, when is necessary, and to take some profile measurement. In order to do this last measurement we used a profilomiter (white-light interferometer) in Swarowski.
At the end of the procedure it should be necessary also to smooth a little bit the surface. In order to do this a soft ablation done with a CO_2 laser should be a good possibility. It's also provided for the future to deposit a high-reflectivity coating.

Cleaving and cleaning the fibers

In order to use the fiber in this experiment, it is necessary to prepare it. The starting tip, for avoiding deformations, should be without defect and without angle tilt. The easier way to obtain it is to cleave the fiber.
The cleaving consists in different steps. As already seen, the fibers we use have a first copper coating and than a titanium one.
First of all it's necessary to remove the copper coating and for doing this there are different chemical possibility. A first possibility is to use a 25% iron (III) chloride ($FeCl_3$) solution at $50°C$ until the coating is no longer visible. A second one is to immerse the fiber in a 25% nitric acid (HNO_3) solution.
Now it is necessary to remove the titanium coating and for doing it exists at least 2 methods. The first is burning the fiber with a lighter or with the heater and the second one is polishing a diamond paste and then cleaning with some acetone.

It is possible to notice that with the first technique the fiber becomes more fragile and so we usually discarded that possibility. Now we properly

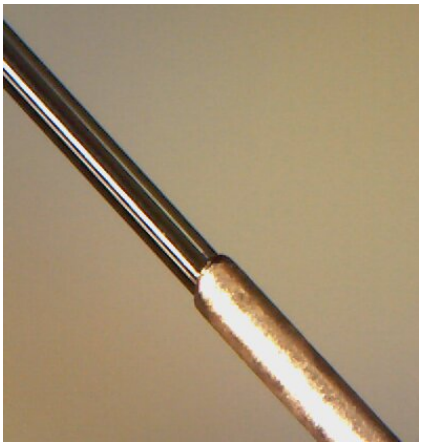

Figure 3.27: Titanium coating after the HNO_3 treatment

cleave the fiber with a cleaving tool. This instrument has two clips for fixing the fiber. Once fixed, one of the two clip is moved back and it is applied a tension depending on the diameter. At this point a ultrasonic vibrating blade is moved onward and backward to apply an accurate cut. This instrument guarantees an angle accuracy in the cut of $\approx 1°$.
For the cleaning of the tip we use a well known procedure. First of all we prepare two clean glasses, one with some acetone and the other one with methanol. Then we put this glasses in an ultrasonic bath at $40°C$ and we leave the fibers for two minutes and an half. It's necessary to take care to not touch the deep end and the border with the fiber because the tip is very delicate and easy to break. In the end we dry it with inert Helium.

Transporting and storing the fibers

It is important also to have some supports for store the fibers. These should avoid that fiber tip:

- touch some rigid support and consequently to break.

- vibrate and possibly breaks because of bending stress.

- get too dirty because exposed to a unclean environment.

Our group is using some aluminium cylinders to solve this issue. These have a central hole and inside there the fibers are posed into a small teflon pipe and fixed with a lateral screw. With these only a small portion of the fiber tip goes out from the holder and so every vibration problem is solved. In any case the tip has to be covered and so it is used an aluminium plate with proper hole where the cylinder are fixed with a screw.

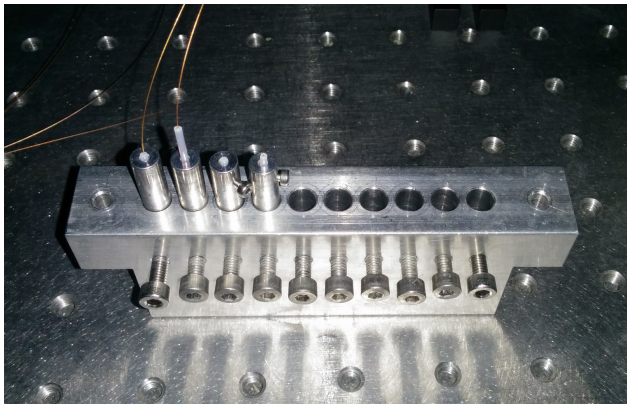

Figure 3.28: Holder for store the fiber. Holed cylinders contain the fibers inside a teflon pipe. These are inserted in holes in a aluminium plates and fixed with a screw

The production procedure

After different tests we choose the following procedure:

1) *Turn on the heater ($T \sim 1600°C$)*
It is necessary to take some precaution in turning on the heater. Indeed it requires high power supply and to avoid damages it is necessary to raise up the current slowly. In particular, we increase the current on the power supply 5 A every two-three minutes until the willed temperature. Then, it is necessary to wait at least half hour for being sure that the temperature is stable.

2) *Mount the fiber and the sphere*
Firstly the sphere is mounted. The pump is turned on and then the ceramic pipe is inserted into the sack where the spheres are stored. Moving properly the sack the right sphere is approached to the end face of the tube and then sucked. It is important to pay attention to the force applied to the tube because it is really easy to break. In the end it is checked with the digital microscope if previous tries has left residual on the sphere.
For the fiber it is firstly put into the first half of the V-groove. Then the fiber is moved until it is outside from the ceramic holder as willed (normally less the $100\mu m$, it is checked approximately by eyes with the microscopes). At this point it is fixed at the end with a clip holder and the other half of the ceramic holder is scrolled up from the bottom in order to avoid that part of the fiber is left outside the V-groove and so pressed and broken. In the end it is clamped with an aluminium plate

and two pressing screws.
At this point fiber and sphere are approached for make easier the next step in the process.

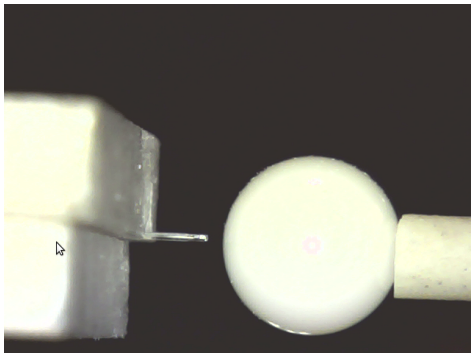

Figure 3.29: Fiber and sphere after the mounting

3) *Align the fiber with the sphere*
Differently from the laser ablation technique where the alignment between laser and the fiber is simply done coupling light of the first into the second, in this experiment it isn't possible. So this operation is done looking at two orthogonal sides of the system with two digital microscopes.
First the center of the sphere is found and this will be discuss in the next paragraph. The second one is properly the alignment which is done manually using the 3D stage. Coupling red light with a fiber tester into the fiber on the sphere may be useful.

4) *Move the heater to the fiber and wait some minutes*
As it has been said before, the heater is moved manually and the position is well determined by two stops fixed to the breadboard. It is important in this step not to touch the heater itself and the metal supports close to it in order to avoid some burning. The region where is safe to handle the holder is signed with blue glue tape as shown in Figure 3.11. It has been seen that the system is ready for the next step after ≈ 10 min.
An important thing to consider is that every part inside the heater is subjected to thermal expansion. In particular it's important to avoid that the fiber touches the sphere because this may damage the surface or misalign these two parts.
A proper initial distance has been evaluate around $500\mu m$.

5) *Using the stages, press the fiber to the sphere*
Also this part is done manually. In this step one of the microscope is completely covered by the heater and so it is possible a partial optical feedback only from the other one. With this microscope it is also difficult to see the fiber-sphere system because of the brightness emitted by the heater but this has been completely solved using proper absorptive filter.
In any case the fiber is pressed until signs of some bending of the fiber are visible. Indeed, because of this bending the signal from the force sensor become completely misleading.

6) *Move back the heater and the fiber*
For this step it has been before removed the heater and then the fiber is separated by the sphere. Only in this way it is possible to avoid to leave some silica glass residual onto the sphere. If there are some visible residuals the sphere is discarded.
After few minutes of cooling down the fiber is removed, checked with the microscope and if it is a good result is stored into the right holder.

The centering

The most limiting factor to produce high quality fiber tips is the alignment (centering). For example with a laser ablation technique this problem is solved by simply coupling the fiber with the laser and it guarantee high accuracy in this sense. In our case the alignment should be done between a fiber and the center of a sphere and so it is impossible to use the previous technique but there are few alternatives. All these will be based on the acquisition of images of the system by a digital microscope.
The first and the most simple possibility should be to overlay a grid to the image acquired from the camera as shown in Figure 3.30. By construction it cannot be too thick and so it isn't so accurate but it is useful for a raw positioning.
Another possibility is to use the back reflection of the sphere and to align it to the fiber. For using this it's necessary to couple a test visible laser light inside the fiber with a fibermeter and than to align the reflection from the sphere with the fiber. The trials with this method in Stuttgart show that it is impossible to join an accuracy smaller than $\sim 100\mu m$.
Finally the last possibility is to use some digital image processing method. For example it is possible to find circular images on the frame.
This last way is the one we used and it will be. It consists in different passages. First of all we need to give to the image a mathematical structure. In

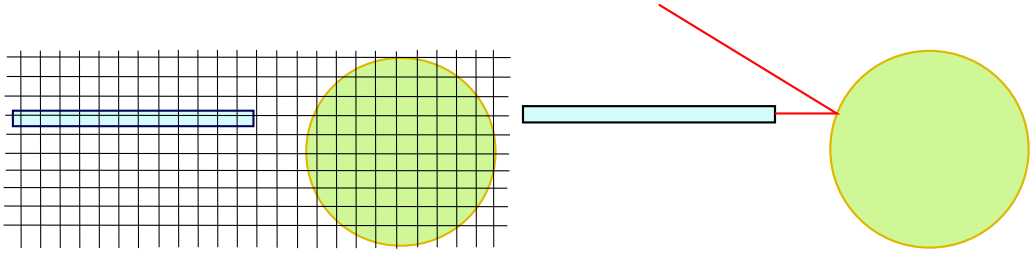

Figure 3.30: Example of raw alignment methods. On the left the grid method and on the right the backreflection one

order to do this it's evident that a color image is inadequate. So first of all we convert the image in a black and white one.
Now we can imagine this as a 2D discrete surface (it has 256 shades of gray and so 256 possible values for a pixel).
This image will have some imperfection due to some focusing error or due to the impossibility to focus every optical ground in the same way (For example in our case we will have a sphere well focused in foreground and the background will be blend). Different techniques to solve the problem (For example the HDR in the new photocamera) but in our case it is not necessary because we are interested in a single object. In any case, this will produce optical noise that can be attenuated with some filter (as a gaussian one).
Now it's important to find out and select only the borders in the image. There are techniques for identifying it:

- Threshold methods: If the image has an high contrast it's possible to identify the edge as the point where there is a discontinuity. It's not possible to use this filter efficiently in every condition.

- First derivative methods (Sobel derivatives): As a 2D surface it's easy to understand that the border will be identified by the inflection points of that. To find that is applied a numerical gradient operator and than identified the maximum of that.

- Second derivative methods (Laplace method): The idea is the same as before but instead of the gradient is applied the Laplacian operator and then the borders are the points in which this derivative is 0.

In the end we chose to apply a Laplacian filter. For finding the center at this point we will use the Hough gradient circle transform. This is a numerical operation which is often used in augmented reality application and, in particular, in digital object identification programs. It is easily possible to

identify with it the two coordinates of the center of the circle and the radius of curvature.

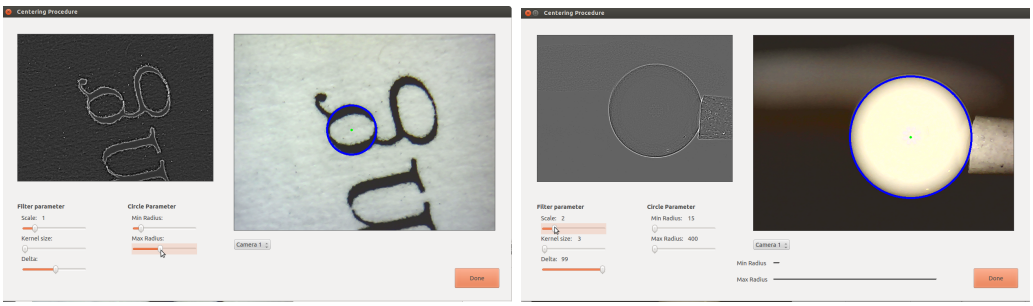

Figure 3.31: Example of the result of this procedure. On the left it is applied on a book page and on the right on our experiment

To sum up our algorithm is composed by the following steps:

- Conversion of the color image from the digital microscope into a black and white one.
- Application of a Gaussian filter in order to reduce the image noise
- Application of the Laplacian filter and identification of the contours of the image
- Hough transform and drawing of the centers

This system has the advantage that it's not required any other instrument and it's legitimate by the fact the a sphere is presented as a circle in every direction you observe it and so, it doesn't suffer of any perspective deformation. The result it's only due to the resolution and the magnification of the digital microscope and to the algorithm. On the other hand it has an high computational cost (solved with a reduction of the frame rate to $\sim$ 24 fps) and some instability due to the probabilistic nature of the Hough transform. The accuracy of this system is around 10 μm.

3.3.3 Results

It has been done a measurement of the profile with a profilometer in Swarowski laboratories in Innsbruck. This sample has been obtained with a temperature $T = 1597 \pm 7°C$ and a sphere in Al_2O_3 of a radius of 1587.5 μm. Below it is shown a typical result.

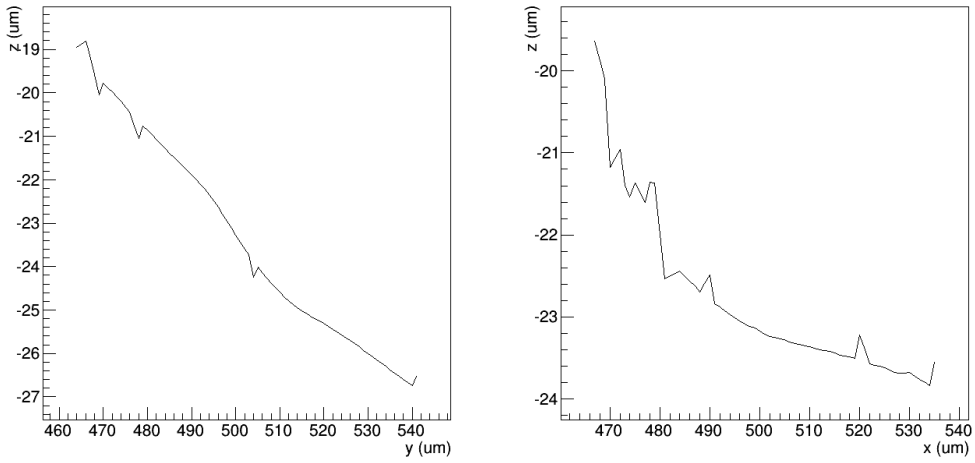

Figure 3.32: Profile section measurement into two orthogonal direction. The concave uncentered profile is evident.

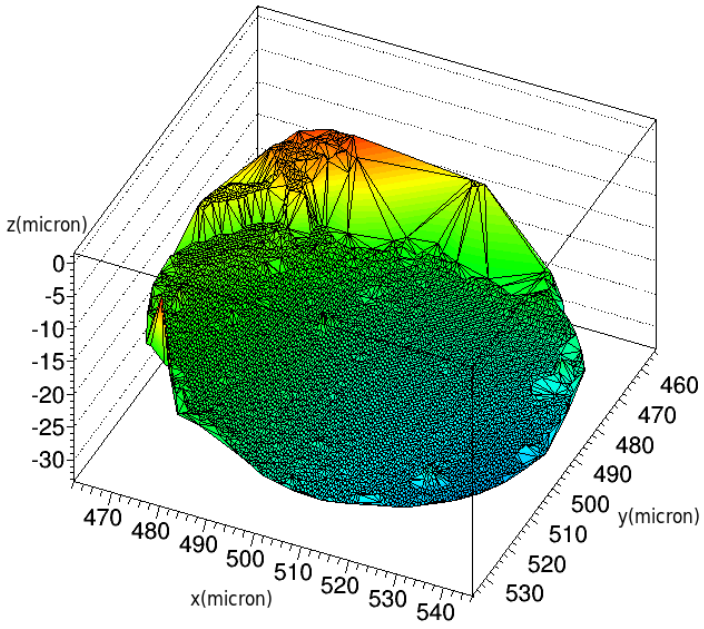

Figure 3.33: 3D Profile of the fiber tip

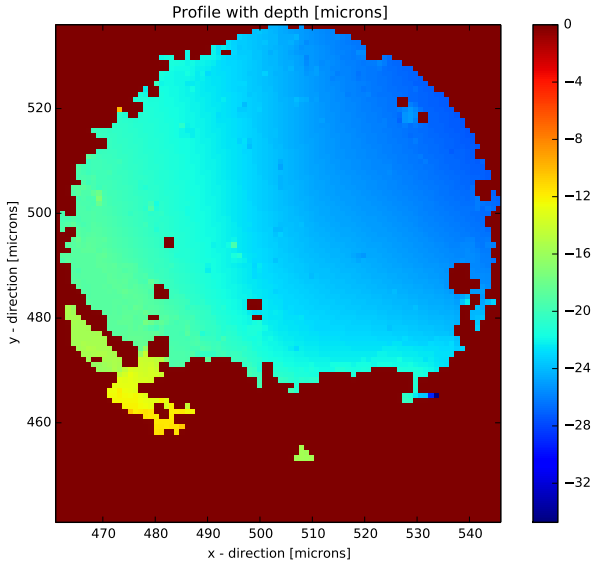

Figure 3.34: 2D plot of the fiber profile of the tip.

Data analysis strategy should involve evidently two steps. The first is the selection of the data. It is evident, indeed, that a portion of the surface hasn't been involved in the process because a bad centering implies that only a part of the surface of the fiber will touch the sphere. So these data has been removed applying a threshold on the z-axis.
Then the analysis has been done with a simple fit with a sphere surface. The function used by fitting is:

$$z = z_0 - \sqrt{R^2 - (x - x_0)^2 - (y - y_0)^2} \tag{3.3.3.1}$$

Where x_0, y_0 and z_0 are the coordinates of the center of the sphere and R is the radius of curvature of the shaped tip.
The result are shown in the table below:

x_0	$536.5 \pm 0.3 \mu m$
y_0	$568.9 \pm 0.2 \mu m$
z_0	$634.44 \pm 0.08 \mu m$
R	$662.18 \pm 0.08 \mu m$

As it is possible to see the profile obtained is concave and this is promising but there are evidently different problem.
The first and more evident question is related the centering: the center is situated out of the fiber profile (of around $100 \mu m$). Even if the algorithm for

the centering used has better performances. The cause of this misalignment has been identified with an not homogeneous deformation of the copper inside the holder in high temperature regime.
The second is related to the surface that, even if concave, shows deviations from the really spherical shape. This is probably due to the not homogeneous temperature inside the heater that causes not linear thermal deformation on the fiber.

Another thing is related with the roughness. The surface shows different

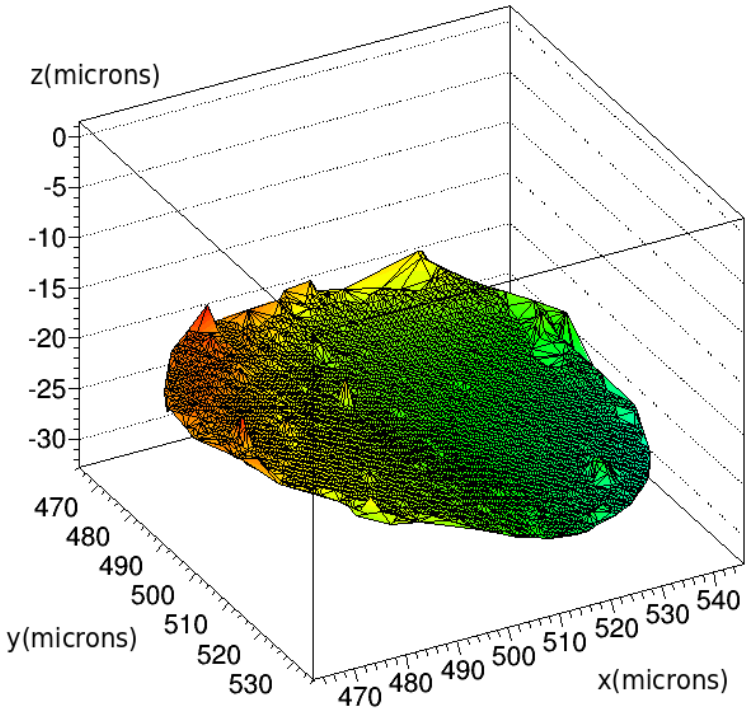

Figure 3.35: The fiber profile after the removing of the outliers with a threshold on z-axis

peaks but probably it is possible to remove it with a weak laser ablation.
The last problem is related to the estimation of the radius of curvature. It is expected that it should be compatible or an overestimation of the radius of curvature of the sphere. This is probably due to three main reasons. The first is probably related to the thermal expansion, it is possible that thermal expansion in the fiber is larger than the one in the spheres. This means that if the fiber tip is imprinted with a certain radius, after the cool down it is decreased, maybe also beyond the one of the sphere. Also contraction after

a so big thermal change may occurs [6]. Exact estimation of this effect are not easy because in this regime of temperature, this material has a not linear behaviour.
A second reason is for sure due to the irregularity of the surface. Indeed, the results changes significantly even if a small portion of data is removed.
These reason may justifies a variation of the radius of around 10%.
The main contribution is related to the glass viscosity. Indeed, in this temperature regime silica glass is characterized by an high viscosity and with Al_2O_3 it becomes adhesive. So when the fiber is moved from the sphere a force arises and deforms the shape of the tip. A possible solution is to change the material of the sphere into one with a lower adhesive coefficient.
It has been shown a maximum gap of $\approx 1\mu m$ from the ideal spherical shape.

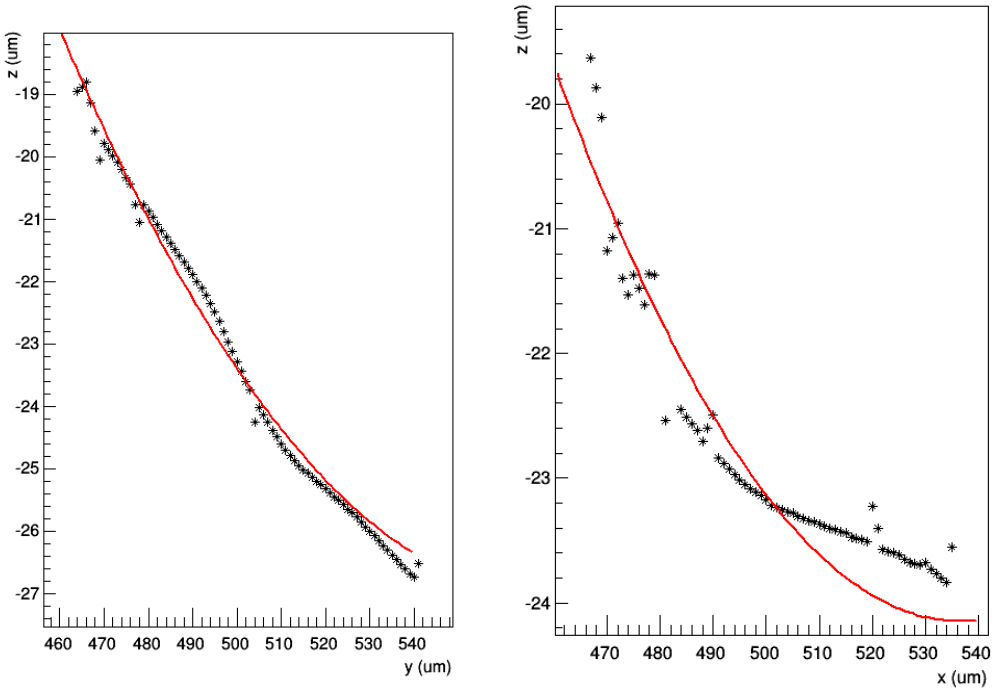

Figure 3.36: Example of profile in orthogonal directions with the fitted profile.

In any case this is only a preliminary result, solving the problem that it will be presented in the next section the hope is to obtain better surfaces.

3.3.4 Problems

The experiment has few problems due to different causes. They can be mainly divided in:

- Problems due to the high temperature and its incompatibility with different material

- Problems due to some mechanical defects or errors.

The first can be easily identified with the enormous difficulty in finding good material for high temperature experimental application in air.
An example of this are the ceramic holder. Ceramic is quiet fragile as material and so it requires replacements quiet often. Only few ceramic are good for our temperature range as it is possible to see in the table below:

Ceramic name	Max temperature (in air)	Machinability
Glass Ceramic	$400 - 600°C$	Depends
MACOR	$800 - 1000°C$ (in air)	Yes
Bisque-fired Alumina	$1427°C$	Yes
Full-fired Alumina	$1649°C$	Yes

Another problem it is evidently related to the machinability. Indeed for optimize the holders is interesting to have the possibility to direct produce the V-groove. In fact, its dimension is not easily predictable, the milling machine has normally accuracy less than $50\mu m$ and so are necessary different trials for obtain optimal results. Even if some alternative are good in terms of material properties these are very technical and so expensive and in this sense are not good in multiple trials. A solution can be the use of ceramic tube that are also exploited in the sphere holder but these will be explained well in the next section.
Another problem is related to the coating of the fibers. It is necessary to ave a vacuum compatible coating and the alternatives are a copper coating or a polymeric one. In the end we choose the copper one because the copper has an higher melting temperature. In fact it presents a couple of disliked behaviour if subjected to this temperature:

- A problem is about the deformation inside the holder. Indeed, the ceramic of the holder, the copper in the coating and the silica glass of the fiber have different thermal expansions coefficient and behaviour. In particular the copper hasn't a homogeneous deformation and this introduce some misalignment during the production which are not easily

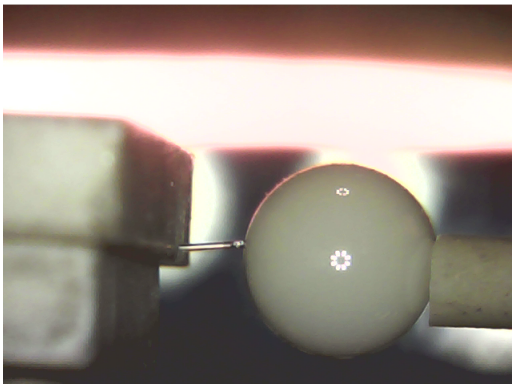

Figure 3.37: Example of the system after an heating up. As it is evident by eyes the fiber is completely misaligned.

solvable because one of the optical access to the experiment is covered by the heater. In Figure 3.37 there is an example of how much severe this problem is and justifies the centering problem in the result.

- Another problem that causes the copper is that overreached a certain temperature ($\sim 600°C$) this material begins to melt down. It often happens that some part of this glue itself on the ceramic support that has been used. The fiber become completely useless and sometimes it's necessary to change the support. It is possible to etch more copper in order to avoid a completely melting but there are cases where the copper leave some residual and dirt on the support, causing the breaking of the fibers in an other trials.

- High temperature may diffuse some atom of Cu into the silica glass and this may change some optical properties of the fiber. We have attributed the loss of transmission of the fiber reasonably to this cause.

- When the copper reaches temperatures near its melting point it oxidises more rapidly. This is not vacuum compatible and it occupies more volume than the previous coating and so it expands also onto the etched part of the fiber as it is possible to see in Figure 3.38. This is glued on the coating but not on the fiber. It is not reactive to HNO_3 acid solution but it is easily removable by hand with a optics cleaning tissue and acetone. On the other hand this procedure may damage the tip and so it is inadvisable.

Another problem related with the temperature involves the fiber glass. Indeed over $1400°C$ the fiber begins to incorporate air showing a sort of peculiar "bubbles" structure. It let the fiber be more fragile and it doesn't

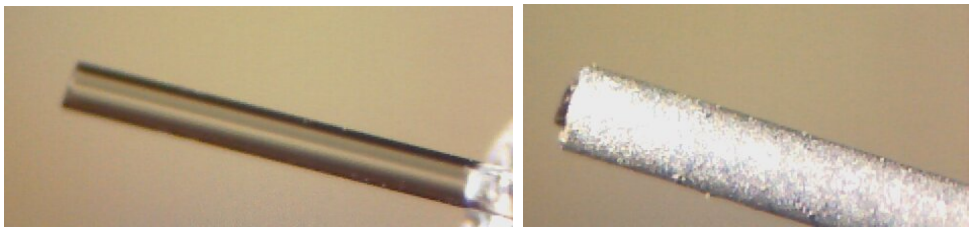

Figure 3.38: Example of the coating oxidation. On the left the fiber before the process, on the right the fiber with the oxidised coating

transmit light anymore.

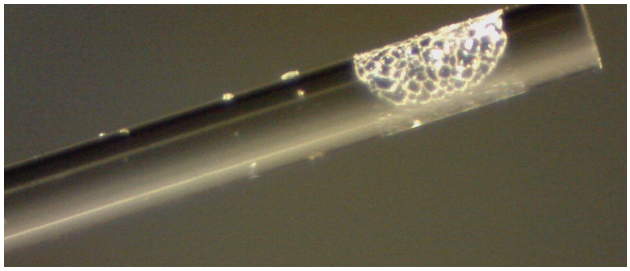

Figure 3.39: Example of this "bubble" problem with the fibers

The experiment has another problem related with the fiber bending. When the fiber is compressed with the stage to the spheres it bends. This has two negative consequences:

- The bending may breaks the fiber. It's not simple and trivial to solve it. Indeed, when the fiber bends, it is hard in every case to identify this problem because it happens with the heater loaded so, not every optical access are available. It can happen that from the perspective of the microscope that is looking at the fiber there is no bending but on the other direction there is.

- The bending makes the signal from the force sensor completely misleading. In fact this effect reduces the force that the sensor can detect below the sensitivity threshold and so induces the experimentalists to increase the pressure when it isn't really necessary and in such way, increasing the risk to break the fiber.

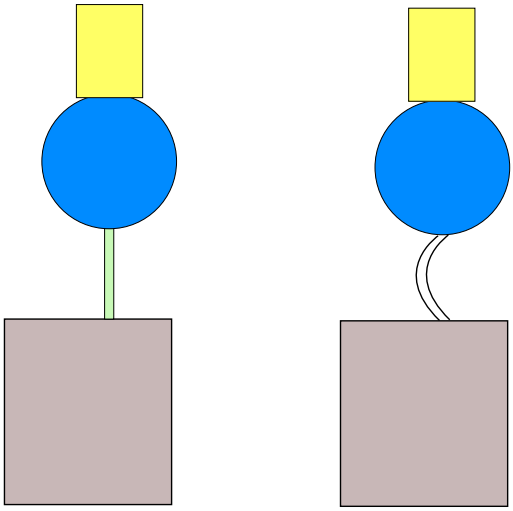

Figure 3.40: Scheme of a standard bending situation. As intuitively understandable if from a direction is evidently bent (on the right) it's not sure that this effect will be visible on the other side

3.3.5 Future developement

There are some evident improvements that are possible to implement in the experiment in order to solve, at least partially, the problems. Furthermore other functionality not related with the problem will be introduced in the next few months for having a very automatic setup.

- **Improvement for solving the problems**
  First of all, the main building problems to solve are the ones related with the material and their thermal properties. Many solutions may be proposed:

  1) A new fiber holder may solve the problem related with the fiber. One solution may be to use the same pipes exploited for the sphere holder which are easy to find in commerce, with various inner and external radius and with adapted thermal properties. Some tests were done with it but the fibers stay glued to the support after the process if not deeply etched because the copper melts down. In any case, a too etched fiber is really fragile because not coated. A solution to this should be to use a ceramic tube with a bunch of fixing fibers inside. This should limit the bending but on the other hand it's not easy to mount and so it's better to find other ways to solve it.

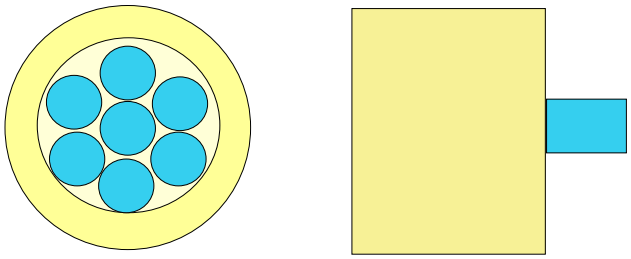

Figure 3.41: Scheme of a bunch of fiber inside the tube. As it's shown the central fiber is constrained by the others. If the tip outside is short this mounting should limit internal and external bending

2) Another solution is to find more performing materials for the supports. A possibility that has proper thermal properties is the zirconia ferrule. It has a melting temperature of $2715°C$, it is machinable and in commerce it is quiet cheap and sold already with a fiber holder design.

3) Another possibility is to change the heating system. Indeed the idea is to reduce the volume involved in the heat up and so a resistive oven isn't a good solution. An alternative is suggested by another device for machining the fibers: the fiber splicer. This device aims to connect two end face of fibers melting them together. The fiber obtained with this tool has a good transmission efficiency.
For integrating either the holder and the heater system it's necessary a really small source of heat. Standard choice for that are electric arc but can also be used a gas flame or tungsten filament through which current passes. The first one guarantees a small heated volume and so only the tip is involved in the process.

- **Improvement for new functionality**
In this sense two proposal has been done.
The first one is to change the heater with the electrical arc based one proposed in the previous point and the holder with zirconia ferrule ones.
At this point new functionalities which are not been implemented yet are the automatic movement for the fiber holder. A motorised tridimensional stage has been already mounted but a digital controller is needed.
It should be also advantageous with a digital controlled system to implement an automatic alignment procedure. In order to do this it's

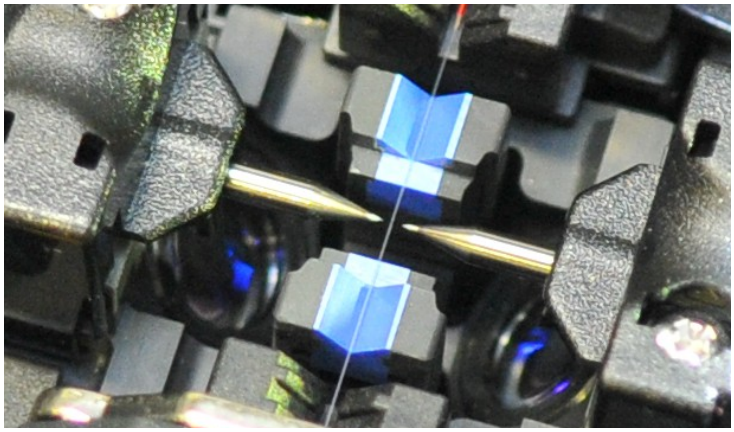

Figure 3.42: A model of fiber splicer. The one in this figure works with an electrical arc between the two metal contact to the side of the fiber (in center)

possible to use a similar algorithm to find the center of the spheres. Indeed it exists a variation of the Hough transform which allows to identify every regular bidimensional shape. In particular, if the cameras are well aligned, the fiber can be approximate to a rectangle.
An example algorithm in order to do that may be composed by the following steps:

1) Find the center of the sphere with the previous technique
2) Find the rectangular border of the fiber. Rotation of the image are not important.
3) Identify the rectangular long axis finding the mean point from the tip pixel to pixel onto the border.
4) Extend this segment to the area which is not covered from the fiber. This will be possible with a fit and in general this won't pass from the center of the sphere.
5) Align this line with the center of the sphere with a digital controller lead by the computer
6) Repeat this procedure for both the axis

A second possibility is to keep the actual setup changing only the holder with the bunch of fiber configuration and to implement what it remains. One big thing is to add the movement control for the heater. For this a project has been already done and it is a modification of a linear rail for a 3D printer.

A sketch of the project is shown in Figure 3.43.

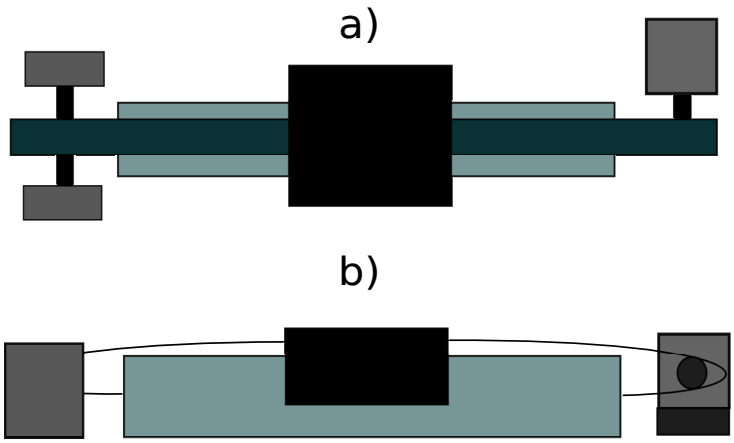

Figure 3.43: A sketch of the linear rail project. a) is a view of the top and b) is a view from in front. To the left an holder for the pulley, to the right the stepper motor. The movement is transmitted with a rubber timing pulley

It modifies the slider of the experiment, connecting the slide side to side with a timing belt and the movement is given by a stepper motor and transfer on the other side of the rail by a pulley.
This complete actuator is controlled by a driver (a circuit that give the correct supply to the motor) lead by a controller (probably always an Arduino Board). Indeed Arduino board cannot supply the correct current (typical value are around $\approx 2A$) without damaging the board itself. A library for controlling a stepper motor it has been already found and it should be possible to reach at least the 1/2 microstepping. Typical step angle are 1.8° and pulley radius of 5 mm and so the movement reproducibility is around 0.1 mm which is enough for our purpose. Indeed it guarantees not to have relevant variation in temperature due to the positioning.

3.3.6 Conclusion

In this thesis it has been shown how cavities are important in optics also in research group today. Cavities may be realise in very different ways but a very interesting implementation is on fiber tips. The way to produce it is usually done in two. A first one in which the end face of fiber are shaped with a concave profile and a second where are coated to give it the proper optical properties.

This project has tried new alternative techniques for machining fiber tips. This application is very important because allow an easier integration of cavity in optical devices and it is particularly useful if exploited in Cavity QED experiments.
In this thesis we have seen that actual laser ablation techniques guarantee very good result in term of surface quality and centering but up to now it is impossible to build spherical cavities with fibers that involve the complete diameter and so it is not possible to build stable cavities of every possible length (larger than $200\mu m$).
Variation of laser ablation has been proposed, each with peculiar problems. A really promising technique is to use a mechanical alternative but differently from the previous fiber machining only few experiences has been done on this. This method provide to press with a ball the end face of a fiber and imprinting its shape when properly heated
A first try of this possibility has been done in Stuttgart in Giessen's reaserch group with non-standard fiber. A modification of that has been proposed in Innsbruck laboratories and it looks quiet promising from the results.
In any case lots of problems has been found and the main causes are the chosen materials for the holders and their high temperature behaviour and the heating system.
Reasonable solutions for that has been thought and in the next few months these will be tested and some definitive result will be desirable.

Bibliography

[1] R. P. Feynman, *There's Plenty of Room at the Bottom*, Engineering and Science, 23 (5), 1960

[2] P. Shor, *Algorithms for quantum computation: discrete logarithms and factoring*, Foundations of Computer Science, 1994 Proceedings., 35th Annual Symposium on, 124 -134, 1994

[3] L. Grover, *A fast quantum mechanical algorithm for database search*, Proceedings of the twenty-eighth annual ACM symposium on Theory of computing, 212-219, 1996

[4] A. K. Ekert, Quantum cryptography based on Bell's theorem, Phys. Rev. Lett. 67, 661-663 (1991)

[5] R. Blatt, T.E. Northup et al., *Integrated Fiber-Mirror Ion Trap for Strong Ion-Cavity Coupling*

[6] D. Hunger, T. Steinmetz, Y. Colombe et al., *A Fabry-Perot cavity with high finesse*, New Journal of Physics 12, 2010

[7] Bahaa E.A. Saleh and Malvin C. Teich, *Fundamental of Photonics*, Wiley, 1991

[8] N. Hodgson and H. Weber, *Optische Resonatoren*, Springer,1992

[9] Wolfgang Demtroeder, *Laser Spectroscopy*, Springer, 1996.

[10] Anthony E. Siegman, *Lasers*, University Science Books, 1986

[11] D.M.B. Kunert, T.P. Meyrath and H. Glessen, *Fabrication of a fiber-based microcavity with spherical concave fiber tips*, Applied Physics B 98, 4(2010)

[12] S. Haroche, J. M. Raimond, *Exploring the Quantum*, Oxford university press, 2006

[13] M. A. Nielsen, I. L. Chuang, *Quantum Computation and Quantum Information*, Cambridge University Press, 2000

[14] W. B. Joyce, B. C. DeLoach, *Alignement of Gaussian beams*, Applied Optics, Vol. 23 No 23, 1984

[15] R. Hauck, H.P. Kortz, H. Waber, *Misalignment sensitivity of optical resonators*, Applied Optics, Vol. 19 No 4, 1980

[16] G. Bradski, A. Kaehler, *Learning OpenCV - Computer vision with OpenCV library*, O'Reilly, 2008

[17] D. Ioannou, W. Huda, A. F. Laine, *Circle recognition through a 2D Hough Transform and radius histogramming*, Image and Vision Computing 17, 15-26, 1999